Available online at www.sciencedirect.com
SCIENCE DIRECT®
Journal of Sound and Vibration 278 (2004) 1095–1129
JOURNAL OF SOUND AND VIBRATION
www.elsevier.com/locate/jsvi

Non-linear stability analysis of a complex rotor/stator contact system

J.-J. Sinou*, F. Thouverez, L. Jezequel

Laboratoire de Tribologie et Dynamique des Systèmes, Equipe Dynamique des Structures et des Systèmes, Ecole Centrale de Lyon, Batiment E6, 36 avenue Guy de Collongue, 69134 Ecully, France

Received 11 October 2002; accepted 23 October 2003

Abstract

In this paper, a non-linear strategy, based on the centre manifold, the rational approximants and the alternating frequency/time domain method has been developed, in order to study the non-linear dynamical behaviour of a system in the neighbourhood of a critical steady state equilibrium point. The stability analysis and the non-linear dynamics of a complex braking system with a non-linear rotor/stator contact are presented. Moreover, one of the most important steps of this paper is the determination of the non-linear behaviour and the limit cycle amplitudes of this complex system. In order to conduct this study, the dynamic response is evaluated by using applying the centre manifold, the rational approximants and the alternating frequency/time domain method, that permit to obtain rapidly and efficiently the non-linear behaviour of the system. The dynamic response obtained by applying this method is compared with that evaluated through numerical integration.

1. Introduction

Non-linear dynamical structures depending on control parameters are encountered in many areas of science and engineering. These systems have to be described by non-linear models due to the fact that they depend strongly on the non-linearities. Under certain conditions, the associated equilibrium point of the non-linear dynamical systems loses stability and small oscillations grow with time. In this case, the non-linearities limit the oscillation growth, and the periodic solutions, called limit cycles, appear. Mathematically speaking, this phenomenon is due to the crossing of the complex plane imaginary axis by a pair of pure imaginary eigenvalues while all other eigenvalues have negative real parts. This type of bifurcation is named Hopf bifurcation [1]. In the

*Corresponding author. Tel.: +33-4-72-18-64-64; fax: +33-4-72-18-91-44.
E-mail address: jean-jacques.sinou@ec-lyon.fr, sinouje@mecasola.ec-lyon.fr (J.-J. Sinou).

0022-460X/$ - see front matter © 2003 Elsevier Ltd. All rights reserved.
doi:10.1016/j.jsv.2003.10.048

study of non-linear dynamical systems depending on a given control parameter, the Hopf bifurcation is one of the most important.

If the conditions and the values of the parameters which cause instability can be investigated with a linear stability theory, there is the need to take into account the complete non-linear expressions in order to obtain the behaviour of the non-linear system and the limit cycle oscillations. Moreover, the understanding of the behaviour of the non-linear models with many degrees of freedom usually requires a simplification and a reduction of the equations; effectively, the non-linear analysis can be rather expensive and consumes considerable resources both in terms of computation time and of data storage requirements. The principal idea for the studies of these dynamical systems is to use simplification methods for reducing the order of the system and eliminating as many non-linearities as possible in the system of equations. One of the frequently used reduction methods is the centre manifold approach. The principle of this non-linear method is based on the reduction of the dimension of the original system: the essential non-linear dynamic system characteristics in the neighbourhood of an equilibrium point are governed by the centre manifold associated with the part of the original system characterized by the eigenvalues with zero real parts at the Hopf bifurcation. Usually, the centre manifold can have complex non-linear terms. In this case, the non-linear system can be simplified by using further non-linear co-ordinate transformations [1–11]. The normal form theory is often applied after the centre manifold approach. The main objective in the method of normal forms is to obtain a simplest possible non-linear system by the use of successive non-linear co-ordinate transformations. At the end of these non-linear transformations, only the resonant terms are retained: they cannot be eliminated and are essential to the non-linear system dynamics. Moreover, there exist methods which combine the centre manifold and the normal form theories into one uniformed procedure [10].

In this paper, the authors choose the use of the rational approximants [12] after applying the centre manifold approach. Moreover, one of the advantages of the rational polynomial approximants can be that they have a greater range of validity than the polynomial one in any case [12–15]. In this paper, the Padé approximants are used in order to simplify the non-linear system. They appear very interesting in regard to computational time; they also necessitate very few computer resources.

In this paper, the authors firstly introduce a non-linear model for brake system with non-linear rotor/stator frictional contact. Secondly, the general mechanisms for friction-induced vibrations are presented in order to find the most suitable mechanism to describe the self-excited vibrations considered in this study. Next, results from stability and parametric studies associated are developed; stability is investigated by determining eigenvalues of the linearized perturbation equations about each steady state operating point. The brake friction coefficient is used as an unfolding parameter of the fundamental Hopf bifurcation point. Finally, the study is concerned with the non-linear dynamic and the determination of the limit cycle amplitudes of the rotor/stator contact system. The centre manifold theory is used in order to reduce the order of the non-linear model in the neighbourhood of an equilibrium point upon bifurcation; the method of the rational polynomial approximants is applied in order to simplify the non-linear equations. Finally, one uses the alternating frequency–time harmonic balance [16] to expand the response of the non-linear dynamical system in their Fourier series. Limit cycles oscillations from centre manifold, rational approximants, and AFT harmonic balance method are compared with the limit cycle oscillations obtained by the integration of the complete set of non-linear dynamics

equations. The main objective is to illustrate the use of non-linear methods for a non-linear system of large dimension in order to obtain rapidly the limit cycles amplitudes of the non-linear system and to show the computational efficiency of these methods. Then, parametric studies for various brake pressure are presented to illustrate the use of the non-linear strategy in order to obtain the evolution of the limit cycles amplitudes.

Therefore, the purpose of this model is the understanding and the detection of the whirl vibration and the associated frictional mechanism. At first, the whirl vibration with the non-linear frictional forces is explained; the non-uniform compression of the stator and the rotor, as well as the frictional force variation on the rubbed stator/rotor interface are concerned. The complex non-linear rotor/stator contact system model related to the whirl vibration will then be discussed.

2. Model of non-linear rotor/stator contact system

The problem of unstable vibrations in disks brakes has received the attention of a number of investigators. Whirl and squeal [17] of disk brake are typical brake vibrations modes and are potentially hazardous types of vibrations which have been observed in several generations of aircraft [17,18]. Whirl can be defined as a wobbling motion between the brake's stationary and the rotating parts. Stationary disks are called stators and rotating disks are called rotors. Whirl vibration usually occurs around 200–500 Hz range. Squeal is a torsional vibration of non-rotating parts of the braking system around the axle. The frequency spectrum of squeal is in the range 100–1000 Hz.

Moreover, a serious difficulty in the study of the dynamic stability of a brake system is the determination of the frictional mechanism. Different types of vibrations induced by friction have been studied in the past by several researchers [19–22]. The different mechanisms of friction-induced vibration fall into four classes: stick-slip, variable dynamic friction coefficient, sprag-slip [23], and geometric coupling of degrees of freedom. The first two approaches rely on changes in the friction coefficient with the relative sliding speed to affect the system stability [24]. The latter two approaches utilize kinematic constraints, and modal coupling to develop instability when the friction coefficient is constant [25–29]. In this study, the authors will consider the latest two approaches that use modal coupling in order to develop instability when the friction coefficient is constant.

In a previous work, Feld and Fehr [30] presented the model defined in Fig. 1, in order to explain the whirl vibration. In this treatment, the instability mechanism is produced by normal force variations that result from dynamic interactions and relative movement of the system degree-of-freedom. The disks are compressed by the hydraulic pressure applied to the brake. Without vibration, the normal pressure is distributed uniformly over the rubbed surface between rotating and stationary disks. When vibration is present, disks in the brake system are subjected to out-of-plane rotation called accordion motion. Then, the uniform normal pressure over the disk interface is altered by this accordion motion: the normal pressure increases over half of the interface and relaxes over the other half. Moreover, the friction force varies proportionally to this normal pressure and produces the whirl motion, as illustrated in Fig. 1.

One assumes that the non-linear normal stress N acting at the interface surface between the rotor and the stator is expressed as a polynomial in the relative displacement normal to the

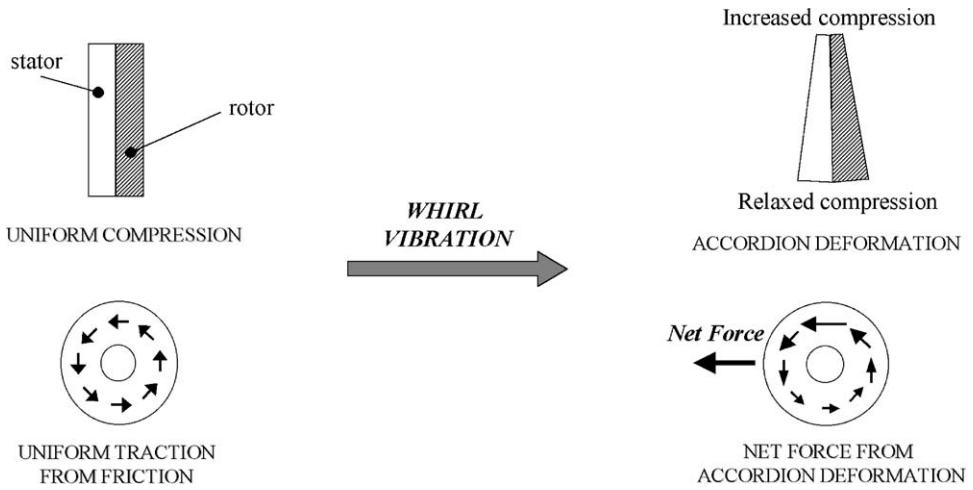

Fig. 1. Friction force variation on rubbed surface.

friction surface. This non-linear normal stress is given by

$$N(r,\theta) = \sum_{i=1}^{3} K_i [x(r,\theta)]^i, \tag{1}$$

where x represents the relative displacement between the rotor and the stator at the point $M(r,\theta)$. K_1, K_2 and K_3 are the linear, quadratic and cubic coefficients of the non-linear contact between the rotor and the stator. The non-linear relationship between load and deflection has been verified by experimental tests conducted on a rotor–stator assemblies [17].

One assumes that the tangential stress T is generated by the brake friction coefficient μ, considering the Coulomb friction

$$T(r,\theta) = \mu N(r,\theta). \tag{2}$$

In this study, the brake friction μ is assumed to be constant. This is due to the fact that there is only a very small variation of the brake friction coefficient during a whirl vibration event, as described by Liu et al. [17]. So the variation of the brake friction coefficient can be assumed to be negligible in this case, although this is not always the case for modelling brake systems. This context is complex enough to be qualitatively predictive and simple enough to allow sensitivity analysis. Here, the retained mechanism to explain the whirl vibration is a classical mechanism; whirl is modelled as a flutter instability due to the non-conservative aspect of Coulomb's friction. Moreover, it is assumed that the rotor and stator friction surfaces are always in contact. For any point $M(r,\theta)$ on the rotor and stator, and by considering small displacements, the normal displacement of the rotor and the stator are

$$\begin{aligned} x_{rotor}(r,\theta) &= x_r - r\sin\theta\sin\theta_r - r\cos\theta\sin\psi_r \approx x_r - r\theta_r\sin\theta - r\psi_r\cos\theta, \\ x_{stator}(r,\theta) &= x_s - r\sin\theta\sin\theta_s - r\cos\theta\sin\psi_s \approx x_s - r\theta_s\sin\theta - r\psi_s\cos\theta, \end{aligned} \tag{3}$$

where x_s, x_r, θ_s, θ_r, ψ_s and ψ_r are the stator and the rotor lateral displacement, and the stator and rotor rotations, as illustrated in Fig. 2.

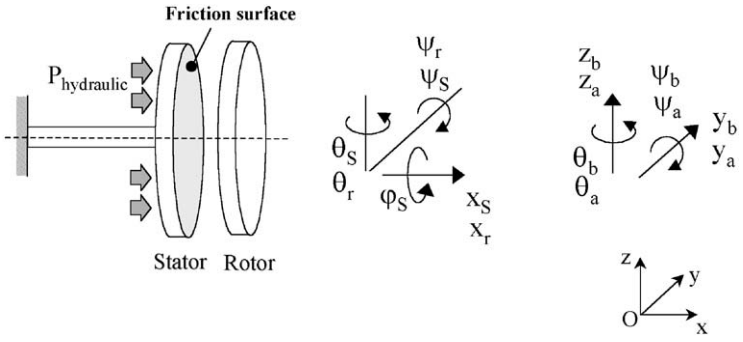

Fig. 2. Dynamic model of rotor/stator braking system.

Then, for any point $M(r,\theta)$ on the disc surface, the normal displacement is

$$x(r,\theta) = x_{stator}(r,\theta) - x_{rotor}(r,\theta) = (x_s - x_r) - r\sin\theta(\theta_s - \theta_r) - r\cos\theta(\psi_s - \psi_r). \tag{4}$$

The normal force F_X due to the normal contact between the rotor and the stator friction surface, and the moment M_X, M_Y and M_Z are given by

$$F_X = \int_0^{2\pi}\int_{R_i}^{R_0} N(r,\theta) r \,\mathrm{d}r\,\mathrm{d}\theta, \tag{5}$$

$$M_X = \int_0^{2\pi}\int_{R_i}^{R_0} T(r,\theta) r^2 \,\mathrm{d}r\,\mathrm{d}\theta = \int_0^{2\pi}\int_{R_i}^{R_0} \mu N(r,\theta) r^2 \,\mathrm{d}r\,\mathrm{d}\theta, \tag{6}$$

$$M_Y = -\int_0^{2\pi}\int_{R_i}^{R_0} N(r,\theta) r^2 \sin\theta \,\mathrm{d}r\,\mathrm{d}\theta, \tag{7}$$

$$M_Z = -\int_0^{2\pi}\int_{R_i}^{R_0} N(r,\theta) r^2 \cos\theta \,\mathrm{d}r\,\mathrm{d}\theta. \tag{8}$$

By considering the previous expressions and expressions (1) and (4), one obtains

$$\begin{aligned} F_X = {} & K_1 A_2 (x_s - x_r) + K_2 (A_2 (x_s - x_r)^2 + \tfrac{1}{4} A_4 (\theta_s - \theta_r)^2 + \tfrac{1}{4} A_4 (\psi_r - \psi_s)^2) \\ & + K_3 (A_2 (x_s - x_r)^3 + \tfrac{3}{4} A_4 (\theta_s - \theta_r)^2 (x_s - x_r) + \tfrac{3}{4} A_4 (\psi_s - \psi_r)^2 (x_s - x_r)), \end{aligned} \tag{9}$$

$$\begin{aligned} M_Y = {} & -\tfrac{1}{4} K_1 (\theta_s - \theta_r) - \tfrac{1}{2} K_2 A_4 (\theta_s - \theta_r)(x_s - x_r) \\ & - K_3 (\tfrac{3}{4} A_4 (\theta_s - \theta_r)(x_s - x_r)^2 + \tfrac{1}{8} A_6 (\theta_s - \theta_r)^3 + \tfrac{1}{8} A_6 (\theta_s - \theta_r)(\psi_s - \psi_r)^2), \end{aligned} \tag{10}$$

$$\begin{aligned} M_X = {} & \mu(\tfrac{2}{3} K_1 A_3 (x_s - x_r) + K_2 (\tfrac{2}{3} A_3 (x_s - x_r)^2 + \tfrac{1}{5} A_5 (\theta_s - \theta_r)^2 + \tfrac{1}{5} A_5 (\psi_s - \psi_r)^2) \\ & + K_3 (\tfrac{2}{5} A_3 (x_s - x_r)^3 + \tfrac{3}{5} A_5 (x_s - x_r)(\theta_s - \theta_r)^2 + \tfrac{3}{5} A_5 (x_s - x_r)(\psi_s - \psi_r)^2)), \end{aligned} \tag{11}$$

$$\begin{aligned} M_Z = {} & -\tfrac{1}{4} K_1 A_4 (\psi_s - \psi_r) - \tfrac{1}{2} K_2 A_4 (\psi_s - \psi_r)(x_s - x_r) \\ & - K_3 (\tfrac{3}{4} A_4 (\psi_s - \psi_r)(x_s - x_r)^2 + \tfrac{1}{8} A_6 (\psi_s - \psi_r)^3 + \tfrac{1}{8} A_6 (\psi_s - \psi_r)(\theta_s - \theta_r)^2) \end{aligned} \tag{12}$$

with $A_k = \pi(R_0^k - R_i^k)$ for $2 \leqslant k \leqslant 6$.

Then, one considers the simple rotor/stator model defined in Fig. 2. It consists of a rigid rotor, a rigid stator, a rotor shaft rigid in torsion, and a stator shaft rigid in torsion. The equations of motion are given in Appendix A and the parameter values in Appendix B.

By considering the non-linear equations of motion in Appendix A, the general form of this non-linear 15-degree-of-freedom system can be expressed in the following way:

$$\mathbf{M}\ddot{\mathbf{x}} + \mathbf{C}\dot{\mathbf{x}} + \hat{\mathbf{K}}\mathbf{x} = \mathbf{F} + \mathbf{F}_{contact}(\mathbf{x}), \tag{13}$$

where $\ddot{\mathbf{x}}$, $\dot{\mathbf{x}}$ and $\mathbf{x}$ are the acceleration, velocity, and displacement response 15-dimensional vectors of the degrees of freedom, respectively. $\mathbf{M}$ is the mass matrix, $\mathbf{C}$ is the damping matrix and $\hat{\mathbf{K}}$ is the stiffness matrix. $\mathbf{F}$ is the vector force due to net brake hydraulic pressure. $\mathbf{F}_{contact}$ contains the linear and non-linear contact force terms at the stator and rotor interface.

3. Stability analysis

To study the stability of the non-linear system modelled in the previous section, the non-linear equations of motion are first linearized about each steady state equilibrium position; then the eigenvalues of these linearized equations of motion are examined. The equilibrium point $\mathbf{x}_0$ is obtained by solving the non-linear static equations for a given net brake hydraulic pressure. This equilibrium point satisfies the following conditions:

$$\hat{\mathbf{K}}\mathbf{x}_0 = \mathbf{F} + \mathbf{F}_{contact}(\mathbf{x}_0). \tag{14}$$

One can notice that there can be more than one steady state operating point at a given net brake hydraulic pressure. The stability is investigated on the linearized equations by assuming small perturbations $\bar{\mathbf{x}}$ about the equilibrium point $\mathbf{x}_0$, where

$$\mathbf{x} = \mathbf{x}_0 + \bar{\mathbf{x}}. \tag{15}$$

The linearized equations for small perturbations about the equilibrium can be written as follows:

$$\mathbf{M}\ddot{\bar{\mathbf{x}}} + \mathbf{C}\dot{\bar{\mathbf{x}}} + \hat{\mathbf{K}}\bar{\mathbf{x}} = \mathbf{F}^L_{contact}(\bar{\mathbf{x}}) \tag{16}$$

with

$$\mathbf{F}^L_{contact}(\bar{\mathbf{x}}) = \sum_{i=1}^{15} \left.\frac{\partial \mathbf{F}_{contact}(\bar{\mathbf{x}})}{\partial \bar{x}_i}\right|_{x_0} \bar{x}_i. \tag{17}$$

The components of $\mathbf{F}^L_{contact}$ are given by

$$\mathbf{F}^L_{contact}(1) = -\mathbf{F}^L_{contact}(5) = -F^L_X, \tag{18}$$

$$\mathbf{F}^L_{contact}(2) = -\mathbf{F}^L_{contact}(6) = -M^L_Y, \tag{19}$$

$$\mathbf{F}^L_{contact}(3) = -\mathbf{F}^L_{contact}(7) = -M^L_Z, \tag{20}$$

$$\mathbf{F}^L_{contact}(4) = M^L_X, \tag{21}$$

$$\mathbf{F}^L_{contact}(i) = 0 \quad \text{for } 8 \leqslant i \leqslant 15, \tag{22}$$

with

$$F_X^L(\bar{\mathbf{x}}) = (K_1A_2 + 2K_2A_2\Delta_x + 3K_3A_2\Delta_x^2 + \tfrac{3}{4}K_3A_4\Delta_\theta^2 + \tfrac{3}{4}K_3A_4\Delta_\psi^2)(\bar{x}_s - \bar{x}_r) + (\tfrac{1}{2}K_2A_4\Delta_\psi + \tfrac{3}{2}K_3A_4\Delta_\psi\Delta_\theta)(\bar{\psi}_s - \bar{\psi}_r) + (\tfrac{1}{2}K_2A_4\Delta_\theta + \tfrac{3}{2}K_3A_4\Delta_\psi\Delta_\theta)(\bar{\theta}_s - \bar{\theta}_r), \quad (23)$$

$$M_X^L(\bar{\mathbf{x}}) = \mu([\tfrac{2}{3}K_1A_3 + \frac{4}{3}K_2A_3\Delta_x + 2K_3A_3\Delta_x^2 + \tfrac{3}{5}K_3A_5\Delta_\theta^2 + \tfrac{3}{5}K_3A_5\Delta_\psi^2](\bar{x}_s - \bar{x}_r) + [\tfrac{2}{5}K_2A_5\Delta_\theta + \tfrac{6}{5}K_3A_5\Delta_\theta\Delta_x](\bar{\theta}_s - \bar{\theta}_r) + [\tfrac{2}{5}K_2A_5\Delta_\psi + \tfrac{6}{5}K_3A_5\Delta_\psi\Delta_x](\bar{\psi}_s - \bar{\psi}_r)), \quad (24)$$

$$M_Z^L(\bar{\mathbf{x}}) = ([-\tfrac{1}{2}K_2A_4\Delta_\psi + \tfrac{3}{2}K_3A_3\Delta_\psi\Delta_x](\bar{x}_s - \bar{x}_r) - \tfrac{1}{4}K_3A_6\Delta_\psi\Delta_\theta(\bar{\theta}_s - \bar{\theta}_r) + [-\tfrac{1}{4}K_1A_4 - \tfrac{1}{2}K_2A_4\Delta_x - \tfrac{3}{4}K_3A_4\Delta_x^2 - \tfrac{1}{7}K_3A_6\Delta_\theta^2 - \tfrac{3}{8}K_3A_6\Delta_\psi^2](\bar{\psi}_s - \bar{\psi}_r)), \quad (25)$$

$$M_Y^L(\bar{\mathbf{x}}) = ([-\tfrac{1}{2}K_2A_4\Delta_\theta + \tfrac{3}{2}K_3A_3\Delta_\theta\Delta_x](\bar{x}_s - \bar{x}_r) - \tfrac{1}{4}K_3A_6\Delta_\psi\Delta_\theta(\bar{\psi}_s - \bar{\psi}_r) + [-\tfrac{1}{4}K_1A_4 - \tfrac{1}{2}K_2A_4\Delta_x - \tfrac{3}{4}K_3A_4\Delta_x^2 - \tfrac{1}{7}K_3A_6\Delta_\psi^2 - \tfrac{3}{8}K_3A_6\Delta_\theta^2](\bar{\theta}_s - \bar{\theta}_r)) \quad (26)$$

with

$$A_k = \pi(R_0^k - R_i^k) \quad \text{for } 2 \leqslant k \leqslant 6,$$

$$\Delta_x = x_{s0} - x_{r0},$$

$$\Delta_\theta = \theta_{s0} - \theta_{r0},$$

$$\Delta_\psi = \psi_{s0} - \psi_{r0}.$$

By considering the relation

$$\mathbf{F}_{contact}^L(\bar{\mathbf{x}}) = \mathbf{K}_{contact}^L\bar{\mathbf{x}}, \quad (27)$$

the linearized system (16) is given by

$$\mathbf{M}\ddot{\bar{\mathbf{x}}} + \mathbf{C}\dot{\bar{\mathbf{x}}} + (\hat{\mathbf{K}} - \mathbf{K}_{contact}^L)\bar{\mathbf{x}} = 0. \quad (28)$$

Now, stability analyses can be performed on the linearized equations for small perturbations at the operating point of the non-linear systems. As long as the real part of all the eigenvalues remains negative, the system is stable. When at least one of the eigenvalues has a positive real part, the dynamical system is unstable. The imaginary part of this eigenvalue represents the frequency of the unstable mode.

Using the base parameters defined previously, simulations have been performed in order to investigate the stability of the non-linear system, with respect to the brake friction coefficient. Moreover, the Hopf bifurcation point, defined by the following conditions:

$$\mathrm{Re}(\lambda_{centre}(\mu))|_{x=\mathbf{x}_0,\mu=\mu_0} = 0 \quad \text{and } \mathrm{Re}(\lambda_{non\text{-}centre}(\mu))|_{x=\mathbf{x}_0,\mu=\mu_0} \neq 0,$$
$$\frac{\mathrm{d}}{\mathrm{d}\mu}(\mathrm{Re}(\lambda(\mu)))\bigg|_{x=\mathbf{x}_0,\mu=\mu_0} \neq 0 \quad (29)$$

occurs at $\mu_0 = 0.41$. The first condition implies that system (28) has a pair of purely imaginary eigenvalues λ_{centre}, while all of the other eigenvalues $\lambda_{non\text{-}centre}$ have non-zero real parts at

($\mathbf{x} = \mathbf{x}_0, \mu = \mu_0$). The second condition of Eq. (29), called a transversal condition, implies a transversal or non-zero speed crossing of the imaginary axis.

The evolution of frequencies and the evolution of the associated real parts associated when the brake friction coefficient is used as a control parameter are shown in Figs. 3 and 4. As shown in Fig. 3, the system is unstable for $\mu > \mu_0$, and stable for $\mu < \mu_0$. Therefore, it is possible to characterize the stability properties of the linearized system by representing the evolution of the eigenvalues with respect to μ in the complex plane, as illustrated in Fig. 5.

This stability analysis indicates that the instability can occur with a constant friction coefficient. Moreover, the frequency ω_0 of the unstable mode, obtained for $\mu = \mu_0$ is near 480 Hz. There is a perfect correlation with experiment tests, whirl vibration being observed in the 200–500 Hz range.

Next, stable and unstable regions versus two parameters can be performed. As illustrated in Figs. 6–10a, stability analysis is a complex problem and can be altered by changes in the brake

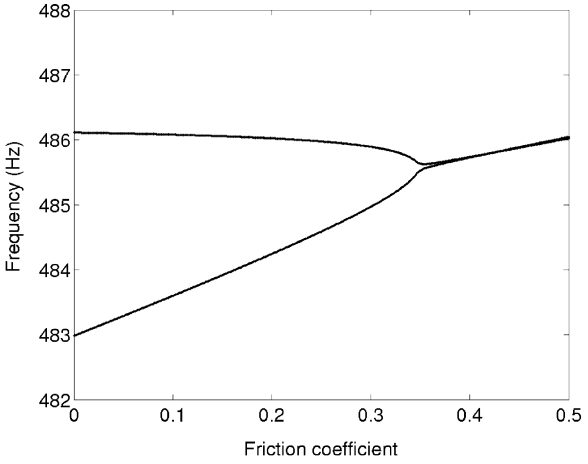

Fig. 3. Coupling of two eigenvalues.

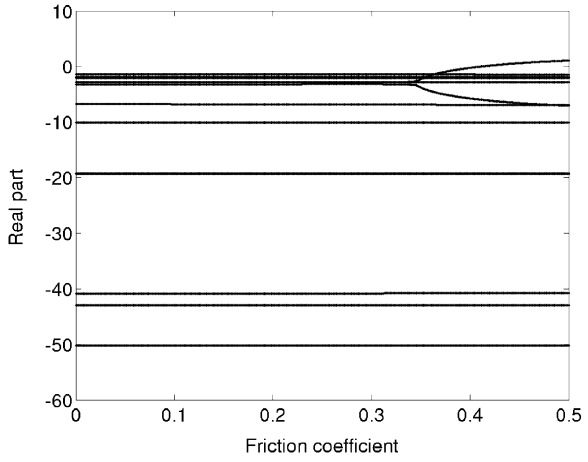

Fig. 4. Evolution of the real part of eigenvalues.

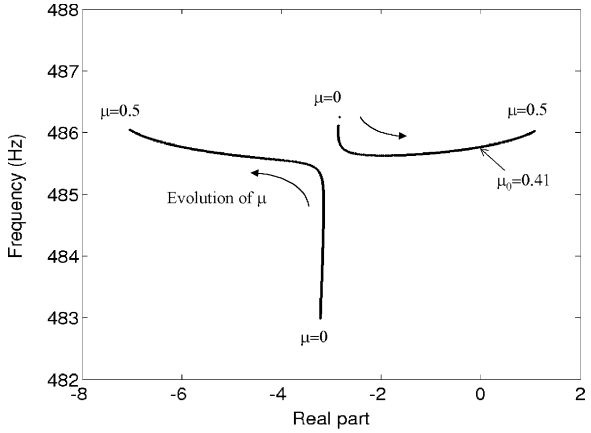

Fig. 5. Evolution of the eigenvalues in the complex plane.

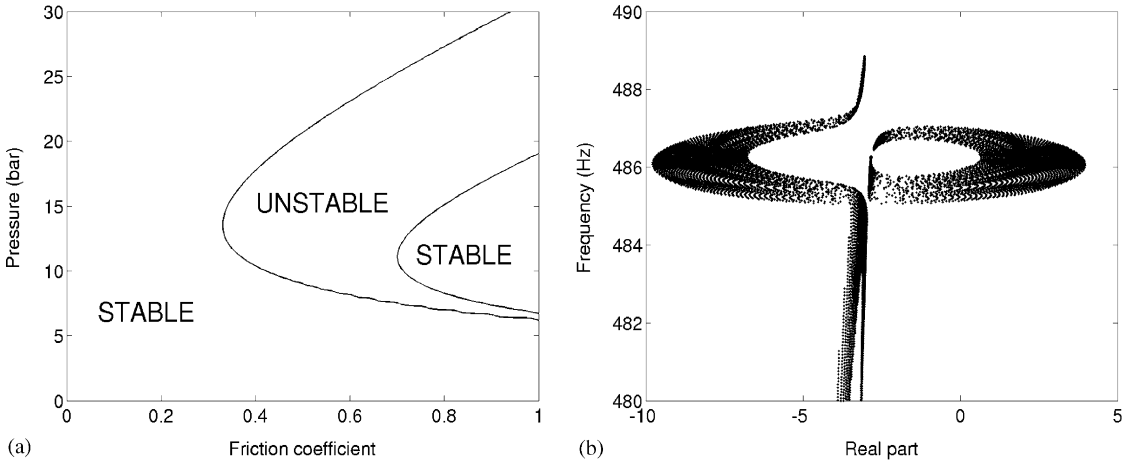

Fig. 6. Stable and unstable regions as a function of the friction coefficient and the pressure.

friction coefficient, the sprag-slip angle, the pressure, or the non-linear rotor/stator contact stiffness. The associated evolutions of the eigenvalues in the complex plane are shown in Figs. 6b to 10b.

4. Non-linear analysis

In order to obtain time-history responses, the complete set of non-linear dynamic equations may be integrated numerically by using the Runge–Kutta method (fourth order), as illustrated in Figs. 11 and 12. But this procedure is both time consuming and costly to perform when parametric design studies are needed. So it is necessary to use non-linear analysis: the centre manifold approach, the rational approximants and the alternate frequency time domain method are used in order to obtain rapidly the limit cycle of the non-linear system.

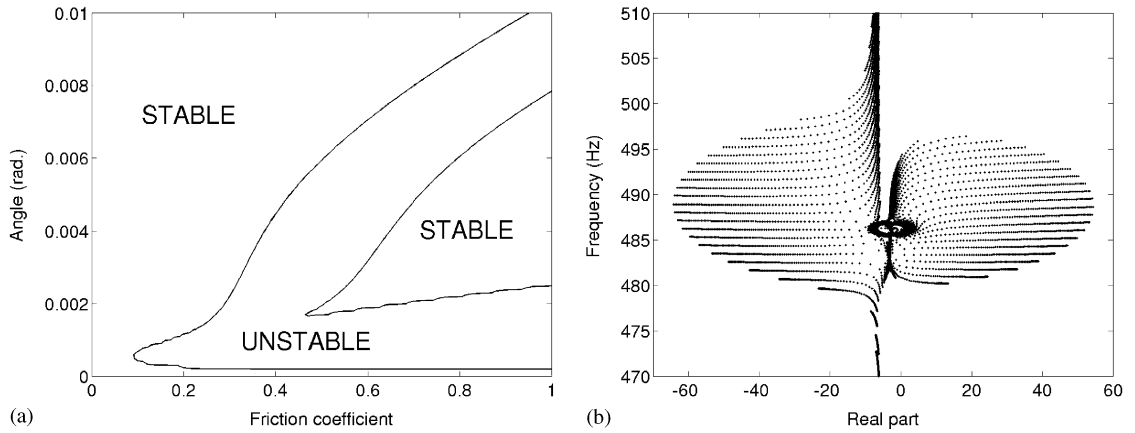

Fig. 7. Stable and unstable regions as a function of the friction coefficient and the sprag-slip angle.

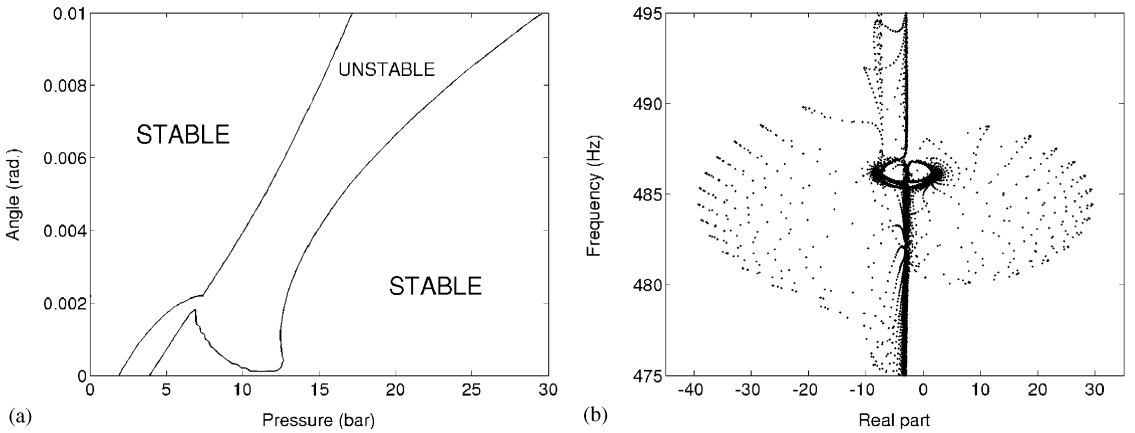

Fig. 8. Stable and unstable regions as a function of the pressure and the sprag-slip angle.

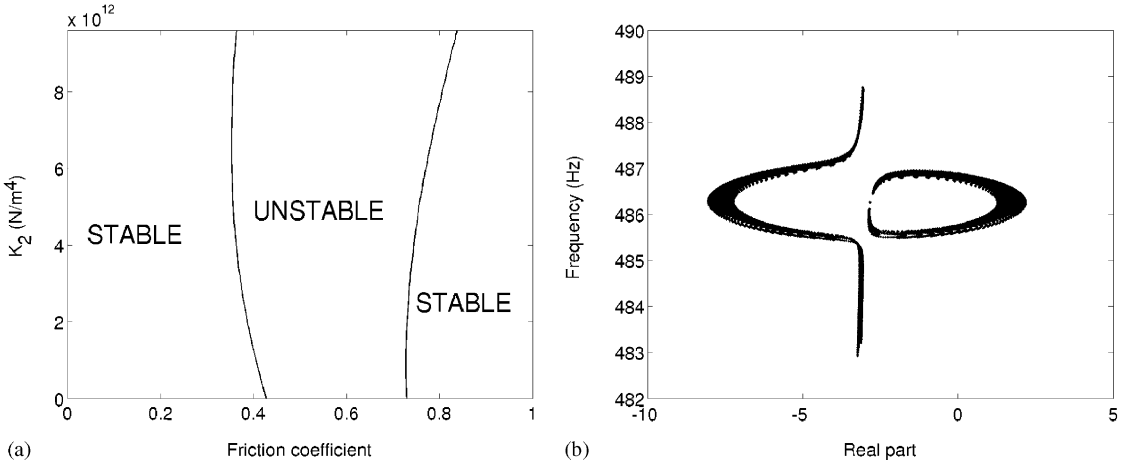

Fig. 9. Stable and unstable regions as a function of friction coefficient and the non-linear stiffness K_2.

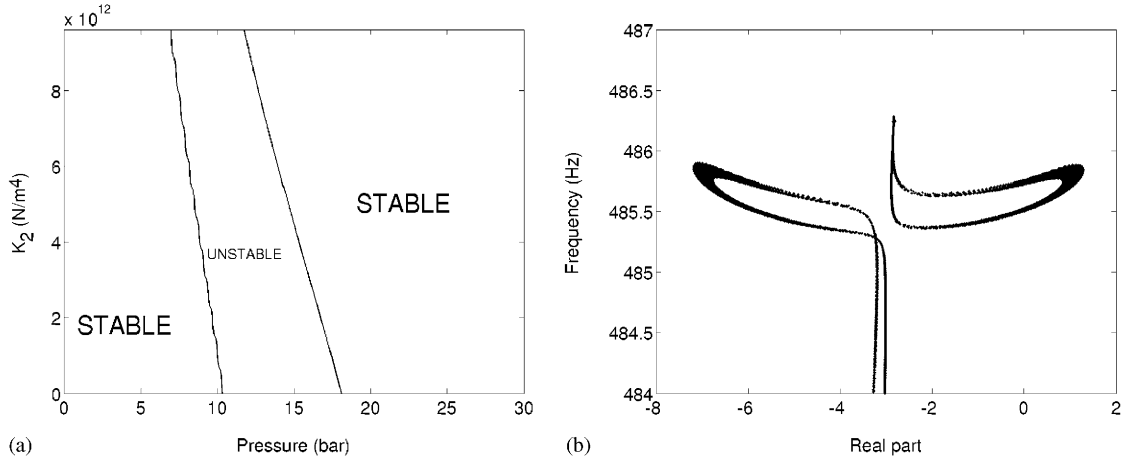

Fig. 10. Stable and unstable regions as a function of the pressure and the non-linear stiffness K_2.

The complete non-linear expressions of the non-linear forces are expressed in order to conduct this complex non-linear analysis. The complete non-linear equations can be written as follows:

$$\mathbf{M}\ddot{\bar{\mathbf{x}}} + \mathbf{C}\dot{\bar{\mathbf{x}}} + \hat{\mathbf{K}}\bar{\mathbf{x}} = \mathbf{F}_{contact}(\bar{\mathbf{x}}), \tag{30}$$

where $\ddot{\bar{\mathbf{x}}}$, $\dot{\bar{\mathbf{x}}}$ and $\bar{\mathbf{x}}$ are the acceleration, velocity, and displacement response 15-dimensional vectors of the degrees of freedom, respectively. $\mathbf{M}$ is the mass matrix, $\mathbf{C}$ is the damping matrix and $\hat{\mathbf{K}}$ is the stiffness matrix. $\mathbf{F}_{contact}(\bar{\mathbf{x}})$ is the non-linear stiffness due to the friction and the rotor/stator contact:

$$\mathbf{F}_{contact}(\bar{\mathbf{x}}) = \mathbf{F}^{L}_{contact}(\bar{\mathbf{x}}) + \mathbf{F}^{NL}_{contact}(\bar{\mathbf{x}}), \tag{31}$$

where the vector $\mathbf{F}^{L}_{contact}$, defined in Eqs. (18)–(22), contains the linear terms of $\mathbf{F}_{contact}$. The vector $\mathbf{F}^{NL}_{contact}$ represents the non-linear terms of $\mathbf{F}_{contact}$ and is given by

$$\mathbf{F}^{NL}_{contact}(1) = -\mathbf{F}^{NL}_{contact}(5) = -F^{NL}_{X}, \tag{32}$$

$$\mathbf{F}^{NL}_{contact}(2) = -\mathbf{F}^{NL}_{contact}(6) = -M^{NL}_{Y}, \tag{33}$$

$$\mathbf{F}^{NL}_{contact}(3) = -\mathbf{F}^{NL}_{contact}(7) = -M^{NL}_{Z}, \tag{34}$$

$$\mathbf{F}^{NL}_{contact}(4) = M^{NL}_{X}, \tag{35}$$

$$\mathbf{F}^{NL}_{contact}(i) = 0 \quad \text{for } 8 \leqslant i \leqslant 15 \tag{36}$$

with

$$\begin{aligned} F^{NL}_{X}(\bar{\mathbf{x}}) = {} & (K_2A_2 + 3K_3A_2\Delta_x)(\bar{x}_s - \bar{x}_r)^2 + \tfrac{3}{2}K_3A_4\Delta_\theta(\bar{\theta}_s - \bar{\theta}_r)(\bar{x}_s - \bar{x}_r) \\ & + \tfrac{3}{2}K_3A_4\Delta_\psi(\bar{\psi}_s - \bar{\psi}_r)(\bar{x}_s - \bar{x}_r) + (\tfrac{1}{4}K_2A_4 + \tfrac{3}{4}K_3A_4\Delta_x)(\bar{\psi}_s - \bar{\psi}_r)^2 \\ & + (\tfrac{1}{4}K_2A_4 + \tfrac{3}{4}K_3A_4\Delta_x)(\bar{\theta}_s - \bar{\theta}_r)^2 + K_3A_2(\bar{x}_s - \bar{x}_r)^3 \\ & + \tfrac{3}{4}K_3A_4(\bar{\theta}_s - \bar{\theta}_r)^2(\bar{x}_s - \bar{x}_r) + \tfrac{3}{4}K_3A_4(\bar{\psi}_s - \bar{\psi}_r)^2(\bar{x}_s - \bar{x}_r), \end{aligned} \tag{37}$$

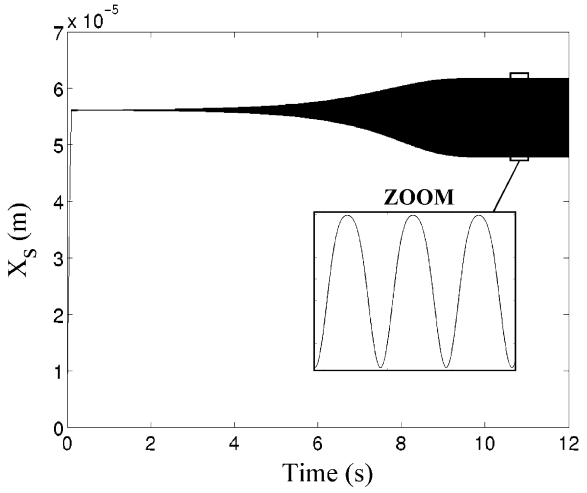

Fig. 11. Evolution of the displacement $X_S(t)$ by using Runge–Kutta 4 ($\mu = 1.1\mu_0$).

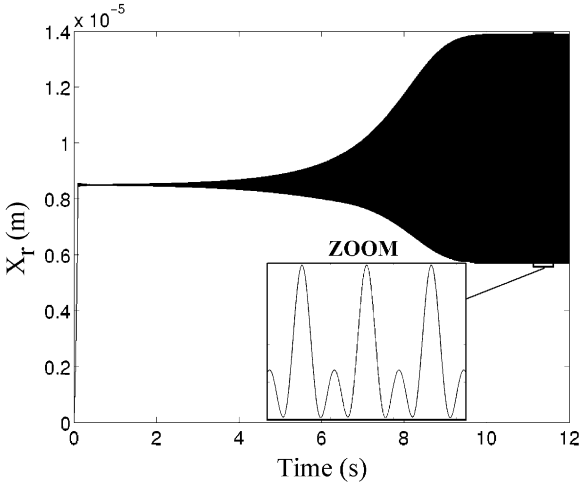

Fig. 12. Evolution of the displacement $X_r(t)$ by using Runge–Kutta 4 ($\mu = 1.1\mu_0$).

$$
\begin{aligned}
M_X^{NL}(\bar{\mathbf{x}}) = \mu([&\tfrac{2}{3}K_2A_3 + 2K_3A_3\Delta_x](\bar{x}_s - \bar{x}_r)^2 + [\tfrac{1}{5}K_2A_5 + \tfrac{3}{5}K_3A_5\Delta_x](\bar{\theta}_s - \bar{\theta}_r)^2 \\
&+ [\tfrac{1}{5}K_2A_5 + \tfrac{3}{5}K_3A_5\Delta_x](\bar{\psi}_s - \bar{\psi}_r)^2 + \tfrac{6}{5}K_3A_5\Delta_\theta(\bar{x}_s - \bar{x}_r)(\bar{\theta}_s - \bar{\theta}_r) \\
&+ \tfrac{6}{5}K_3A_5\Delta_\psi(\bar{x}_s - \bar{x}_r)(\bar{\psi}_s - \bar{\psi}_r) + \tfrac{2}{3}K_3A_3(\bar{x}_s - \bar{x}_r)^3 \\
&+ \tfrac{3}{5}K_3A_5(\bar{\theta}_s - \bar{\theta}_r)^2(\bar{x}_s - \bar{x}_r) + \tfrac{3}{5}K_3A_5(\bar{\psi}_s - \bar{\psi}_r)^2(\bar{x}_s - \bar{x}_r)),
\end{aligned} \tag{38}
$$

$$
\begin{aligned}
M_Y^{NL}(\bar{\mathbf{x}}) = &-\tfrac{3}{4}K_3A_4\Delta_\theta(\bar{x}_s - \bar{x}_r)^2 - \tfrac{3}{8}K_3A_6\Delta_\theta(\bar{\theta}_s - \bar{\theta}_r)^2 - \tfrac{1}{8}K_3A_6\Delta_\theta(\bar{\psi}_s - \bar{\psi}_r)^2 \\
&- (\tfrac{1}{2}K_2A_4 + \tfrac{3}{2}K_3A_4\Delta_x)(\bar{x}_s - \bar{x}_r)(\bar{\theta}_s - \bar{\theta}_r) - \tfrac{3}{8}K_3A_6\Delta_\psi(\bar{\theta}_s - \bar{\theta}_r)(\bar{\psi}_s - \bar{\psi}_r) \\
&+ \tfrac{1}{8}K_3A_6(\bar{\theta}_s - \bar{\theta}_r)^3 + \tfrac{3}{4}K_3A_4(\bar{\theta}_s - \bar{\theta}_r)(\bar{x}_s - \bar{x}_r)^2 + \tfrac{1}{8}K_3A_6(\bar{\theta}_s - \bar{\theta}_r)(\bar{\psi}_s - \bar{\psi}_r)^2,
\end{aligned} \tag{39}
$$

$$
\begin{aligned}
M_Z^{NL}(\bar{\mathbf{x}}) = & -\tfrac{3}{4}K_3A_4\Delta_\psi(\bar{x}_s-\bar{x}_r)^2-\tfrac{3}{8}K_3A_6\Delta_\psi(\bar{\psi}_s-\bar{\psi}_r)^2-\tfrac{1}{8}K_3A_6\Delta_\psi(\bar{\theta}_s-\bar{\theta}_r)^2\\
& -(\tfrac{1}{2}K_2A_4+\tfrac{3}{2}K_3A_3\Delta_x)(\bar{x}_s-\bar{x}_r)(\bar{\psi}_s-\bar{\psi}_r)-\tfrac{3}{8}K_3A_6\Delta_\psi(\bar{\theta}_s-\bar{\theta}_r)(\bar{\psi}_s-\bar{\psi}_r)\\
& +\tfrac{1}{8}K_3A_6(\bar{\psi}_s-\bar{\psi}_r)^3+\tfrac{3}{4}K_3A_4(\bar{\psi}_s-\bar{\psi}_r)(\bar{x}_s-\bar{x}_r)^2+\tfrac{1}{8}K_3A_6(\bar{\psi}_s-\bar{\psi}_r)(\bar{\theta}_s-\bar{\theta}_r)^2 \qquad (40)
\end{aligned}
$$

with

$$A_k=\pi(R_o^k-R_i^k)\quad \text{for } 2\leqslant k\leqslant 6,$$

$$\Delta_x=x_{s0}-x_{r0},$$

$$\Delta_\theta=\theta_{s0}-\theta_{r0},$$

$$\Delta_\psi=\psi_{s0}-\psi_{r0}.$$

By considering expressions (37)–(40), the non-linear equations can be expressed as

$$\mathbf{M}\ddot{\bar{\mathbf{x}}}+\mathbf{C}\dot{\bar{\mathbf{x}}}+(\hat{\mathbf{K}}-\mathbf{K}_{contact}^L)\bar{\mathbf{x}}=\mathbf{F}_{contact}^{NL}(\bar{\mathbf{x}})=\sum_{i=1}^{15}\sum_{j=1}^{15}\mathbf{q}_{(2)}^{ij}\bar{x}_i\bar{x}_j+\sum_{i=1}^{15}\sum_{j=1}^{15}\sum_{k=1}^{15}\mathbf{q}_{(3)}^{ijk}\bar{x}_i\bar{x}_j\bar{x}_k, \qquad (41)$$

where the vectors $\mathbf{q}_{(2)}^{ij}$ and $\mathbf{q}_{(3)}^{ijk}$ are the coefficients of the quadratic and cubic terms due to the non-linear stiffness about the equilibrium point, respectively.

In order to use the non-linear methods (the centre manifold approach and the rational approximants), one writes the non-linear equation in state variables $\mathbf{y}=\{\bar{\mathbf{x}}\ \ \dot{\bar{\mathbf{x}}}\}^{\mathrm{T}}$

$$\dot{\mathbf{y}}=\mathbf{A}\mathbf{y}+\sum_{i=1}^{30}\sum_{j=1}^{30}\mathbf{p}_{(2)}^{ij}y_iy_j+\sum_{i=1}^{30}\sum_{j=1}^{30}\sum_{k=1}^{30}\mathbf{p}_{(3)}^{ijk}y_iy_jy_k, \qquad (42)$$

where y_i defines the ith term of $\mathbf{y}\cdot\mathbf{A}$, $\mathbf{p}_{(2)}^{ij}$ and $\mathbf{p}_{(3)}^{ijk}$ are the 30×30 matrix, quadratic and cubic non-linear terms, respectively. One has

$$\mathbf{A}=-\begin{bmatrix}\mathbf{0} & \mathbf{I}\\ \mathbf{M}^{-1}(\hat{\mathbf{K}}-\mathbf{K}_{contact}^L) & -\mathbf{M}^{-1}\mathbf{C}\end{bmatrix}, \qquad (43)$$

$$\mathbf{p}_{(2)}=\begin{Bmatrix}\mathbf{0}\\ \mathbf{M}^{-1}\mathbf{q}_{(2)}\end{Bmatrix}, \qquad (44)$$

$$\mathbf{p}_{(3)}=\begin{Bmatrix}\mathbf{0}\\ \mathbf{M}^{-1}\mathbf{q}_{(3)}\end{Bmatrix}. \qquad (45)$$

5. The centre manifold approach

Reduction to lower dimensional problem by means of the centre manifold theory is now considered. The centre manifold approach is based on the idea that all essential non-linear stability and dynamic system characteristics in the neighbourhood of an equilibrium point are

governed by the dynamics on the centre manifold, when some eigenvalues have zero real parts and all other eigenvalues have negative real parts.

In a first step, one will express the non-linear system (42) in the new modal linear basis of its eigenvectors, and consider the coefficient of friction as a new variable in order to be able to carry out some sensitivity analysis. One obtains

$$\begin{aligned}
&\dot{\mathbf{v}}_c = \mathbf{J}_c(\hat{\mu})\mathbf{v}_c + \mathbf{G}(\mathbf{v}_c, \mathbf{v}_s, \hat{\mu}),\\
&\dot{\mathbf{v}}_s = \mathbf{J}_s(\hat{\mu})\mathbf{v}_s + \mathbf{H}(\mathbf{v}_c, \mathbf{v}_s, \hat{\mu}),\\
&\dot{\hat{\mu}} = 0,
\end{aligned} \tag{46}$$

where $\mathbf{v}_c \in \mathbb{R}^2$ and $\mathbf{v}_s \in \mathbb{R}^{n-2}$ (with $n = 30$ in this case). System (46) depends on the control parameter $\hat{\mu}$. By considering the physically interesting case of the stable equilibrium loosing stability, one can assume that $\mathbf{v}_c$ contains the two variables associated to the eigenvalues λ with zero real parts, while $\mathbf{v}_s$ contains those with negative real parts. $\mathbf{G}$ and $\mathbf{H}$ are polynomial non-linear functions. At $(\mathbf{v}_c, \mathbf{v}_s, \hat{\mu}) = (0, 0, 0)$, this system has a three-dimensional centre manifold tangent to $(\mathbf{v}_c, \hat{\mu})$ space. The centre manifold theory allows the expression of the variables $\mathbf{v}_s$ as a function of $\mathbf{v}_c$: $\mathbf{v}_s = \mathbf{h}(\mathbf{v}_c, \hat{\mu})$. This $(n-2)$-dimensional function $\mathbf{h}$ is substituted into the second equation of Eq. (46); then these results are combined with the first equation of Eq. (46). By considering the tangency conditions at the fixed point $(0, 0, 0)$ to the centre eigenspace, one obtains

$$\begin{aligned}
&D_{v_c,\hat{\mu}}(\mathbf{h}(\mathbf{v}_c, \hat{\mu}))(\mathbf{J}_c\mathbf{v}_c + \mathbf{G}(\mathbf{v}_c, \mathbf{h}(\mathbf{v}_c, \hat{\mu}), \hat{\mu})) - \mathbf{J}_s\mathbf{h}(\mathbf{v}_c, \hat{\mu}) - \mathbf{H}(\mathbf{v}_c, \mathbf{h}(\mathbf{v}_c, \hat{\mu}), \hat{\mu}) = 0,\\
&\mathbf{h} = \mathbf{0},\\
&D_{v_c}h_i(0) = \mathbf{0} \quad \text{for } 1 \leqslant i \leqslant n-2,\\
&\frac{\partial \mathbf{h}}{\partial \hat{\mu}} = 0,
\end{aligned} \tag{47}$$

where h_i $(1 \leqslant i \leqslant n-2)$ are the scalar components of $\mathbf{h}$. To solve Eq. (47), one defines an approximate solution of $\mathbf{h}$ by a power expansion: one assumes $\mathbf{v}_s = \mathbf{h}(\mathbf{v}_c, \hat{\mu})$ as a power series in $(\mathbf{v}_c, \hat{\mu})$ of degree m, without constant and linear terms $(m \geqslant 2)$:

$$\mathbf{v}_s = \mathbf{h}(\mathbf{v}_c, \hat{\mu}) = \sum_{p=i+j+l=2}^{m} \sum_{j=0}^{p} \sum_{l=0}^{p} \mathbf{a}_{ijl} v_{c1}^i v_{c2}^j \hat{\mu}^l, \tag{48}$$

where $\mathbf{a}_{ijl}$ are vectors of constant coefficients. Substituting the assumed polynomial approximations into Eq. (47), one obtains a system of algebraic equations for the coefficients of the approximate solution of $\mathbf{h}$. The analytical expressions for the coefficients of second and third order polynomial approximation of $\mathbf{v}_s = \mathbf{h}(\mathbf{v}_c, \hat{\mu})$ are given in Appendix C.

After the identification of $\mathbf{h}$, it is resubstituted into the first equation of Eq. (46) in order to obtain the reduced order structural dynamic model, which is only a function of $\mathbf{v}_c$:

$$\begin{aligned}
&\dot{\mathbf{v}}_c = \mathbf{J}_c(\hat{\mu})\mathbf{v}_c + \mathbf{G}(\mathbf{v}_c, \mathbf{h}(\mathbf{v}_c, \hat{\mu}), \hat{\mu}),\\
&\dot{\hat{\mu}} = 0.
\end{aligned} \tag{49}$$

This reduced system is easier to study than the original one. In this centre manifold analysis, one reduces the dynamics of the considered 31-dimensional system to the dynamics on the three-dimensional centre manifold.

In this study, one will obtain the limit cycles only near the Hopf bifurcation point ($\mu = \mu_0 + \bar{\mu}$, where μ_0 is the friction coefficient at the Hopf bifurcation point and $\bar{\mu} = \varepsilon\mu_0$ with ε very small). In this case, one observes numerically that the expressions of $\mathbf{v}_s = \mathbf{h}(\mathbf{v}_c, \bar{\mu})$ can be approximated by the expression of $\mathbf{v}_s = \mathbf{h}(\mathbf{v}_c)$ with negligible errors. This approximation amounts to the expression of $\mathbf{v}_s$ at the Hopf bifurcation point μ_0 ($\mathbf{a}_{ijl} \equiv 0$ for $l \neq 0$). It is not necessary, but nevertheless it allows the simplification of the expression of $\mathbf{v}_s$. Therefore, the non-linear terms are approximated by their evaluation at the bifurcation point $\mu = \mu_0$, provided that none of the leading non-linear terms vanish here; so one has $\mathbf{G}(\mathbf{v}_c, \mathbf{h}(\mathbf{v}_c), \mu) \approx \mathbf{G}(\mathbf{v}_c, \mathbf{h}(\mathbf{v}_c), \mu_0)$ with negligible error due to the fact that ε is very small.

Finally, the dynamics of the system is described, with small errors, by the system

$$\begin{aligned} &\dot{\mathbf{v}}_c = \mathbf{J}_c(\mu)\mathbf{v}_c + \mathbf{G}(\mathbf{v}_c, \mathbf{v}_s, \mu_0), \\ &\dot{\mu} = 0, \\ &\mathbf{v}_s = \mathbf{h}(\mathbf{v}_c) = \sum_{p=i+j=2}^{m} \sum_{j=0}^{p} \mathbf{a}_{ij} v_{c1}^{i} v_{c2}^{j}. \end{aligned} \tag{50}$$

Using an approximation of $\mathbf{h}$ up to the second order is sufficient in order to obtain the evolutions of limit cycle amplitudes. In Figs. 13–15, the limit cycle amplitudes obtained via the centre manifold approach are compared with the ones obtained via the integration of the full system. The comparison of the two approaches shows a good and sufficient correlation. Consequently, the centre manifold approach is validated and reduces the number of equations of the original system from 31 to 3 in order to obtain a simplified system.

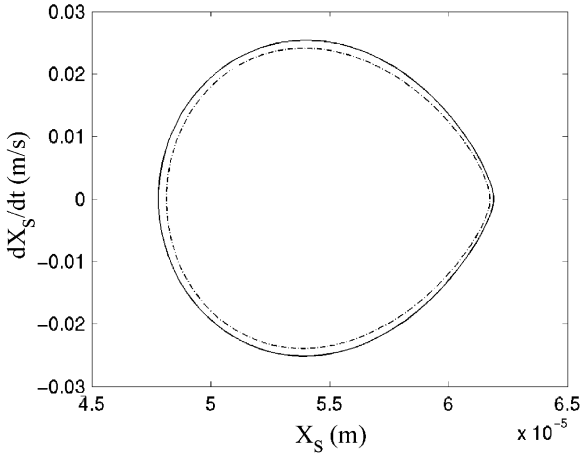

Fig. 13. X_s-limit cycle amplitudes by using the centre manifold approach ($\mu = 1.1\mu_0$); — original system, - - - center manifold approach.

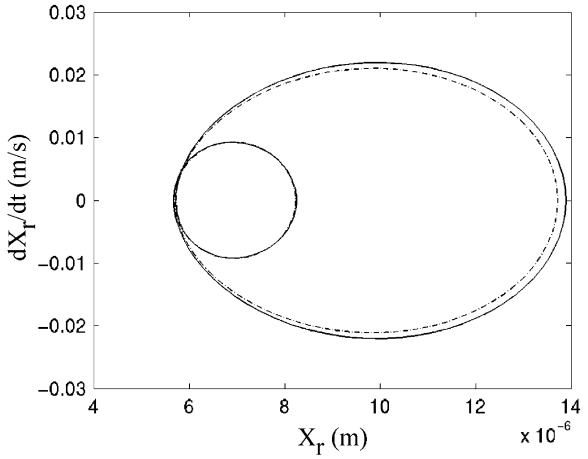

Fig. 14. X_r-limit cycle amplitudes by using the centre manifold approach ($\mu = 1.1\mu_0$); — original system, - - - center manifold approach.

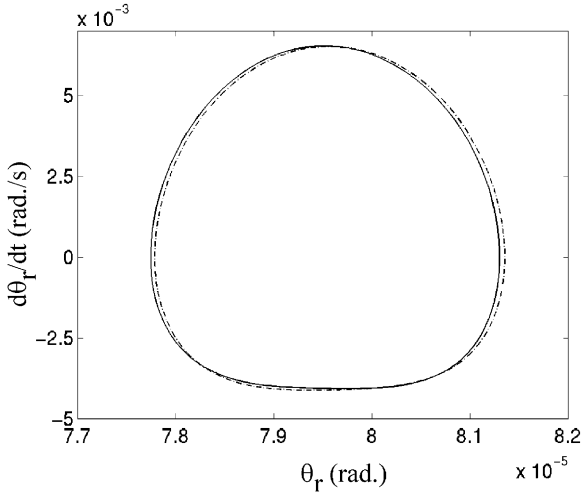

Fig. 15. θ_r-limit cycle amplitudes by using the centre manifold approach ($\mu = 1.1\mu_0$); — original system, - - - center manifold approach.

6. Rational polynomial approximants

In this section, one will use the rational approximants in order to simplify the non-linear system, without losing the dynamics of the original system, as well as the contributions of non-linear terms. The use of the rational approximants allows one to obtain limit cycles more easily and rapidly. The Padé approximants appear very interesting in regard to computational time; they also necessitate very few computer resources.

The main objective in the rational approximants is the approximation of the non-linear terms by using rational polynomial approximants [12,13]. Moreover, one of the interesting things about these rational approximants is that they need less terms than the associated Taylor series in order to obtain an accurate approximation of the limit cycle amplitudes: they allow the computation of an accurate approximation of the non-linear function $f(\mathbf{v}_c)$ even at values of f for which the Taylor series of $f(\mathbf{v}_c)$ diverge. In any case, the rational approximation has a greater range of validity than the polynomial one.

Let $f(x,y)$ be a function of 2-variables defined by a formal power series expansion

$$f(x,y)=\sum_{i=0}^{\infty}\sum_{j=0}^{\infty}c_{ij}x^iy^j=\sum_{(i,j)\in S}c_{ij}x^iy^j, \tag{51}$$

where $S=\{(i,j)\,|\,i\in\mathbb{N}^+,\ j\in\mathbb{N}^+\}$.

In this paper, on considers symmetric-off-diagonal (SOD) rational approximants [12,15] to $f(x,y)$ of the form

$$[M/N]_f(x,y)=\frac{\sum_{(i,j)\in S_M}n_{ij}x^iy^j}{\sum_{(i,j)\in S_N}d_{ij}x^iy^j}, \tag{52}$$

where $S_M=\{(i,j)\,|\,0\leqslant i\leqslant M,0\leqslant j\leqslant M\}$ and $S_N=\{(i,j)\,|\,0\leqslant i\leqslant N,\ 0\leqslant j\leqslant N\}$. There are $(M+1)^2+(N+1)^2$ unknown coefficients in Eq. (52). d_{00} can be normalised to unity and the other coefficients n_{ij} and d_{ij} are then related by matching terms in Eqs. (51) and (52). By multiplying the difference between $f(x,y)$ and $[M/N]_f(x,y)$ by the denominator of $[M/N]_f(x,y)$, one obtains

$$\left(\sum_{(i,j)\in S_N}d_{ij}x^iy^j\right)\times\left(\sum_{(i,j)\in S}c_{ij}x^iy^j\right)-\sum_{(i,j)\in S_M}n_{ij}x^iy^j=\sum_{(i,j)\in S}e_{ij}x^iy^j, \tag{53}$$

where as many coefficients e_{ij} as possible are equal to zero. The equations obtained by matching coefficients in Eq. (53) are

$$d_{00}=1, \tag{54}$$

$$\sum_{i=0}^{\alpha}\sum_{j=0}^{\beta}d_{ij}c_{\alpha-i;\beta-j}=n_{\alpha\beta}\quad\text{for } 0\leqslant\alpha\leqslant M,\ 0\leqslant\beta\leqslant M, \tag{55}$$

$$\sum_{i=0}^{\alpha}\sum_{j=0}^{N}d_{ij}c_{\alpha-i;\beta-j}=0\quad\text{for } 0\leqslant\alpha<M,\ M<\beta\leqslant M+N-\alpha, \tag{56}$$

$$\sum_{i=0}^{N}\sum_{j=0}^{\beta}d_{ij}c_{\alpha-i;\beta-j}=0\quad\text{for } M<\alpha\leqslant M+N-\beta,\ 0\leqslant\beta<M, \tag{57}$$

$$\sum_{i=0}^{\sigma}\sum_{j=0}^{N}(d_{ij}c_{\sigma-i;M+N+1-\sigma-j}+d_{ij}c_{M+N+1-\sigma-i;\sigma-j})=0\quad\text{for } 1\leqslant\sigma\leqslant N. \tag{58}$$

After normalizing d_{00} to unity, the computation of the coefficients d_{ij} can be achieved by solving the linear equations which arise from Eqs. (56)–(58). Next, the linear equations given by Eqs. (55) enable the determination of the coefficients n_{ij}, with the coefficients d_{ij} found previously.

If one considers that the expressions $\mathbf{G}(\mathbf{v}_c, \mathbf{h}(\mathbf{v}_c), \mu_0)$ of Eq. (50) are power series in $\mathbf{v}_c$ of degree $3m$ respectively, then the dynamic of Eq. (50) can be rewritten in the following way:

$$\dot{\mathbf{v}}_c = \mathbf{f}(\mathbf{v}_c) = \sum_{p=1}^{3m} \sum_{i=0}^{p} \mathbf{c}_{i,p-i} v_{c1}^{i} v_{c2}^{p-i}, \tag{59}$$

where m defines the degree of the power series $\mathbf{h}$ in Eq. (50).

By using the SOD rational approximants, the previous system can be written as follows:

$$\dot{\mathbf{v}}_c = \mathbf{f}^{NL}(\mathbf{v}_c) = \left\{ \begin{array}{c} \dfrac{\sum_{i=0}^{M} \sum_{j=0}^{M} n_{1.ij} v_{c1}^{i} v_{c2}^{j}}{\sum_{i=0}^{N} \sum_{j=0}^{N} d_{1.ij} v_{c1}^{i} v_{c2}^{j}} \\ \dfrac{\sum_{i=0}^{M} \sum_{j=0}^{M} n_{2.ij} v_{c1}^{i} v_{c2}^{j}}{\sum_{i=0}^{N} \sum_{j=0}^{N} d_{2.ij} v_{c1}^{i} v_{c2}^{j}} \end{array} \right\}. \tag{60}$$

The determinations of the coefficients $n_{1.ij}$, $n_{2.ij}$ (for $0 \leqslant i \leqslant M$ and $0 \leqslant j \leqslant M$) and $d_{1.ij}$, $d_{2.ij}$ (for $0 \leqslant i \leqslant N$ and $0 \leqslant j \leqslant N$) are obtained using the procedure defined previously.

In addition, one uses the alternate frequency/time (AFT) harmonic balance method. The vector $\mathbf{v}_c(t)$ can be expanded as a truncated Fourier series

$$\mathbf{v}_c(t) = \mathbf{V}_0 + \sum_{j=1}^{H} \left(\mathbf{V}_{2j-1} \cos\left(\frac{2\pi j t}{T}\right) + \mathbf{V}_{2j} \sin\left(\frac{2\pi j t}{T}\right) \right), \tag{61}$$

where T is the period of the system, $\mathbf{V}_0$, $\mathbf{V}_{2j-1}$ and $\mathbf{V}_{2j}$ the vectors of Fourier coefficients. The number of harmonic coefficients H will be selected in order to consider only the significant harmonics expected in the solution. By considering Eqs. (60) and the Fourier expansion (61), one obtains the linear algebraic equations

$$\Delta \mathbf{V}^k = -(\mathbf{A} - \mathbf{J})^{-1} (\mathbf{F}^{NL} + (\mathbf{A} - \mathbf{J}) \mathbf{V}^k), \tag{62}$$

$$\mathbf{V}^{k+1} = \mathbf{V}^k + \Delta \mathbf{V}^k, \tag{63}$$

where $\mathbf{V}^k = \{\{\mathbf{V}_0^k\}^{\mathrm{T}}, \ldots, \{\mathbf{V}_{2j-1}^k\}^{\mathrm{T}}, \{\mathbf{V}_{2j}^k\}^{\mathrm{T}}, \ldots, \{\mathbf{V}_{2H}^k\}^{\mathrm{T}}\}^{\mathrm{T}}$. $\mathbf{V}^k$ defines the k-incremental vector of Fourier coefficients of $\mathbf{v}_c$. $\mathbf{A}$ and $\mathbf{J}$ are the Jacobian matrices associated with the linear and non-linear parts of the equation of motion (60), respectively. $\mathbf{F}^{NL}$ represents the vector of the Fourier coefficients of the non-linear function $\mathbf{f}^{NL}$, defined in Appendix D. The vector of the Fourier coefficients $\mathbf{F}^{NL}$ is calculated by an iteration process [16], by considering the discrete Fourier transform (DFT). This process can be sketched as

$$\mathbf{V} \xrightarrow{\mathrm{DFT}^{-1}} \mathbf{v}_c(\mathbf{t}) \rightarrow \mathbf{f}^{NL}(\mathbf{t}) \xrightarrow{\mathrm{DFT}} \mathbf{F}^{NL}. \tag{64}$$

The error vector $\mathbf{R}$ is given by

$$\mathbf{R} = \mathbf{A}\mathbf{V}^{k+1} - \mathbf{F}^{NL}, \tag{65}$$

and the associated convergences are given by

$$\delta_1 = \sqrt{\mathbf{R}_0^2 + \sum_{j=1}^{H} (\mathbf{R}_{2j-1}^2 + \mathbf{R}_{2j}^2)} \quad \text{and} \quad \delta_2 = \sqrt{\Delta\mathbf{V}_0^2 + \sum_{j=1}^{H} (\Delta\mathbf{V}_{2j-1}^2 + \Delta\mathbf{V}_{2j}^2)}. \tag{66}$$

The complete scheme of the computer program using the alternate frequency/time domain (AFT) method with the DFT is expressed in Fig. 16.

The $[3/2]_f(\mathbf{v}_c)$ symmetric-off-diagonal rational approximants are applied in order to simplify the non-linear expression of the non-linear equation (59), that is a power series in $\mathbf{v}_c$ of degree 6. An $[M/N]_f(\mathbf{v}_c)$ approximation with $L \leqslant 2$ and $M \leqslant 2$ is not sufficient: effectively, in some cases, computations diverge since the retained non-linearities are not sufficient, and in other cases, the obtained limit cycle amplitudes are not acceptable due to the same reasons.

In addition, the first order of harmonic coefficients ($H = 1$) allows one to obtain the same limit cycle amplitudes as those obtained by the integration of the system defined with the

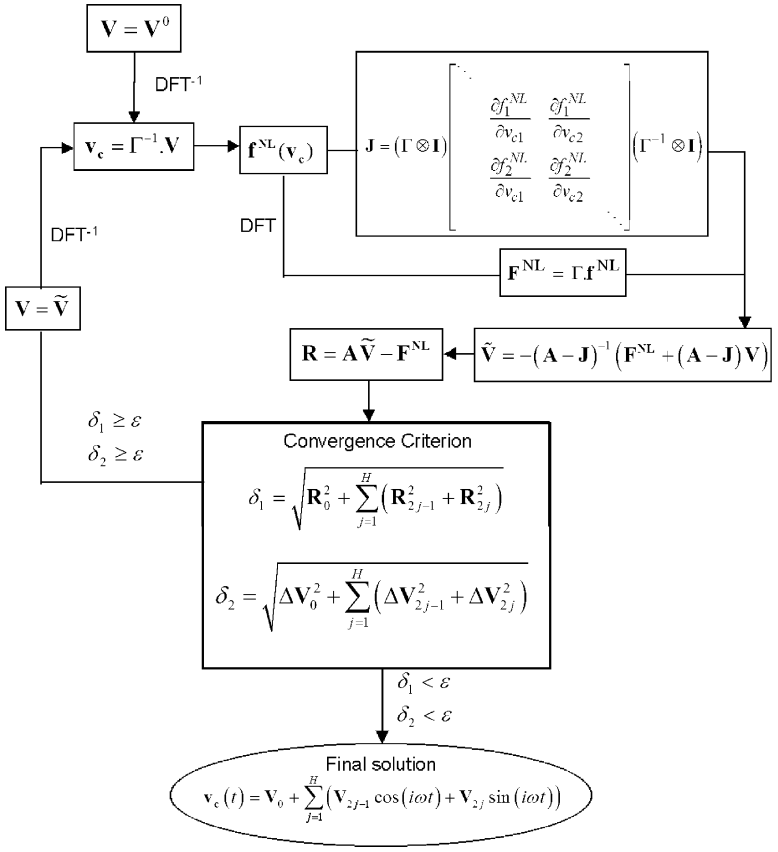

Fig. 16. Description of the AFT method.

Table 1
Vectors of the harmonic coefficients

Vector of the harmonic coefficient	Case 1 ($H = 1$)	Case 2 ($H = 2$)
$\mathbf{V}_0$	$\begin{Bmatrix} -0.0005 - 0.0004\mathrm{i} \\ -0.0005 + 0.0004\mathrm{i} \end{Bmatrix}$	$\begin{Bmatrix} -0.0005 - 0.0004\mathrm{i} \\ -0.0005 + 0.0004\mathrm{i} \end{Bmatrix}$
$\mathbf{V}_1$	$\begin{Bmatrix} 0.4918 - 0.4924\mathrm{i} \\ 0.4918 + 0.4924\mathrm{i} \end{Bmatrix}$	$\begin{Bmatrix} 0.4927 - 0.4933\mathrm{i} \\ 0.4927 + 0.4933\mathrm{i} \end{Bmatrix}$
$\mathbf{V}_2$	$\begin{Bmatrix} 0.4923 + 0.4916\mathrm{i} \\ 0.4923 - 0.4916\mathrm{i} \end{Bmatrix}$	$\begin{Bmatrix} 0.4932 + 0.4925\mathrm{i} \\ 0.4932 - 0.4925\mathrm{i} \end{Bmatrix}$
$\mathbf{V}_3$	$\mathbf{0}$	$\begin{Bmatrix} 0.0001 \\ 0.0001 \end{Bmatrix}$
$\mathbf{V}_4$	$\mathbf{0}$	$\begin{Bmatrix} 0.0001\mathrm{i} \\ -0.0001\mathrm{i} \end{Bmatrix}$

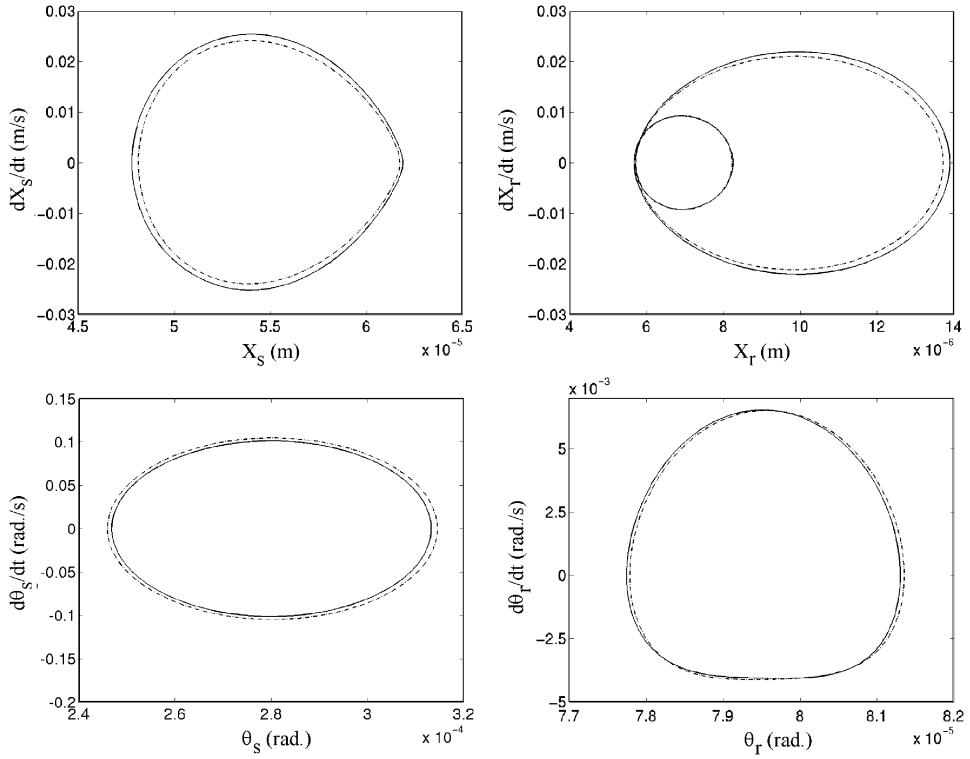

Fig. 17. X_s, X_r, θ_s and θ_s-limit cycles by using the centre manifold, the rational approximants and the alternating frequency/time method ($\mu = 1.1\mu_0$); — original system, -·- non-linear mathods.

$[3/2]_f(\mathbf{v}_c)$ symmetric-off-diagonal rational approximants. The Padé approximants appear very interesting in regard to computational time; they also necessitate very few computer resources.

The values of the harmonic coefficients for one and two harmonics are given in Table 1. Moreover, the values of the harmonic coefficients are complex, since they defined the unknown functions in time of $\mathbf{v}_c$ by their Fourier components in the centre manifold base. Using the reverse transformation in order to go from the centre manifold space (with complex variable) to the physical space (with real variable), one obtains the limit cycle amplitudes of the non-linear physical system.

As illustrated in Figs. 17–20, good correlations between the limit cycles of the integrated system, and those of the $[3/2]_f(\mathbf{v}_c)$ rational approximants and the AFT method are obtained. Consequently, the rational approximants approach is validated and allows the reduction of the number of non-linear terms of the system.

Moreover, the determination of the limit cycle amplitudes by the integration of the differential–algebraic equations of the system is faster using the multivariable approximants. These non-linear methods are ideal for parametric studies.

Some indications have been observed by varying the pressure parameter, as illustrated in Figs. 21 and 22. The friction coefficient is used as the control parameter and the limit cycles are

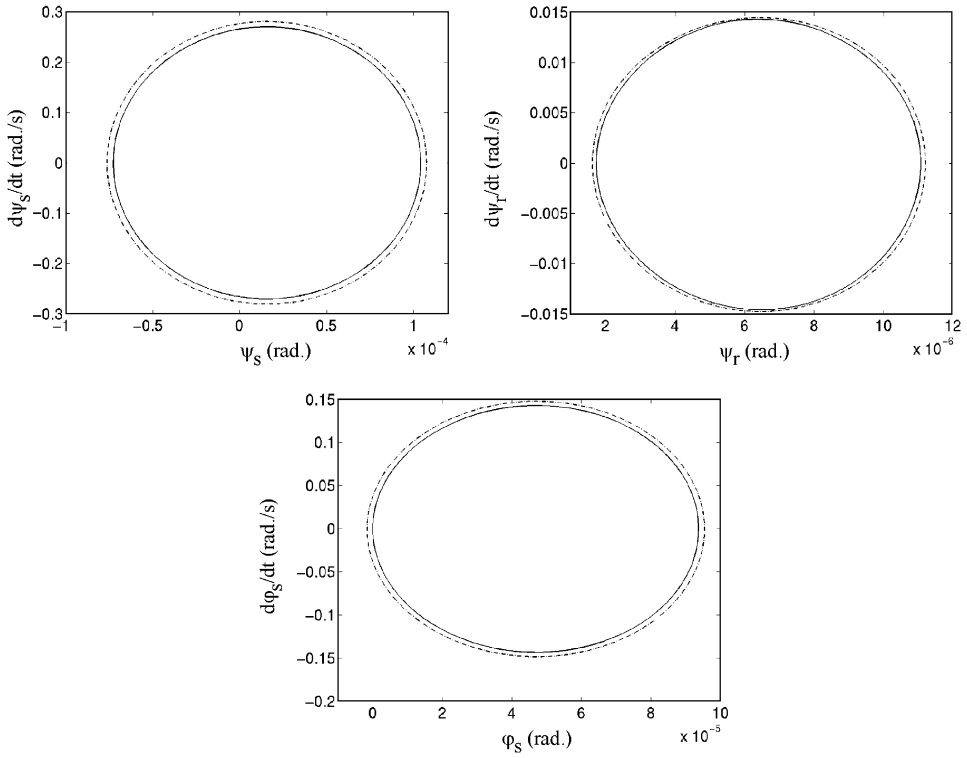

Fig. 18. ψ_s, ψ_r and φ_s-limit cycles by using the centre manifold, the rational approximants and the alternating frequency/time method ($\mu = 1.1\mu_0$); — original system, - · - non-linear mathods.

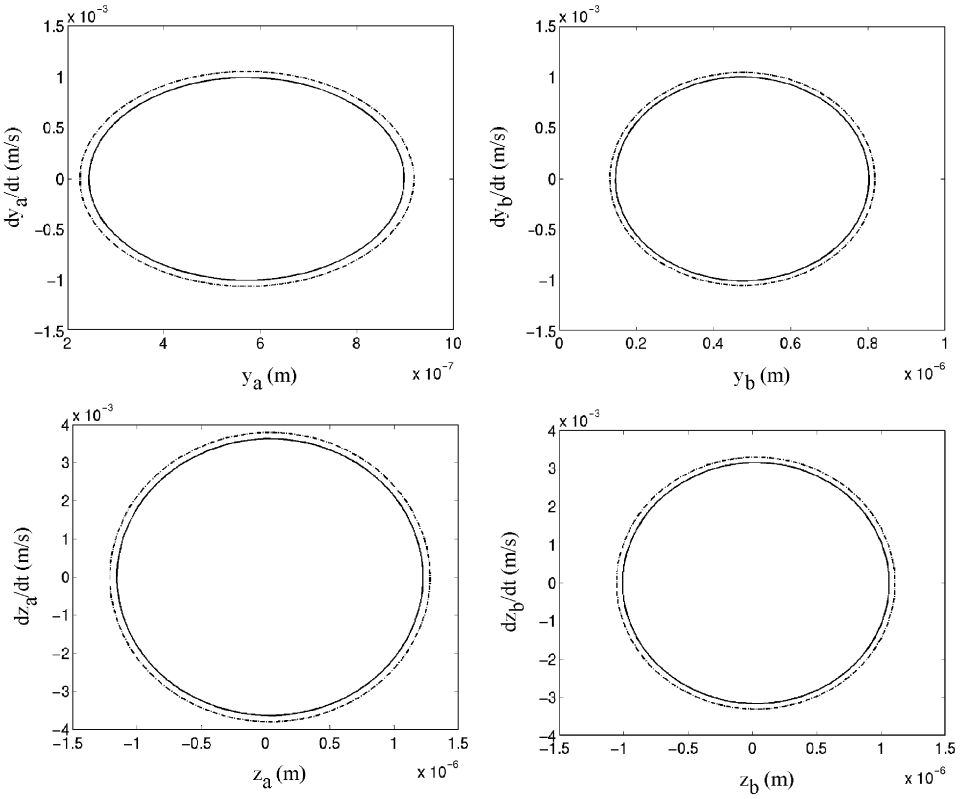

Fig. 19. y_a, y_b, z_a and z_b-limit cycles by using the centre manifold, the rational approximants and the alternating frequency/time method ($\mu = 1.1\mu_0$); — original system, -·- non-linear mathods.

defined near the Hopf bifurcation point. The Hopf bifurcation points are given in Table 2. An evolution of the equilibrium point is observed and the evolution of limit cycles appears to be a complex problem.

7. Summary and conclusion

In this study, the stability analysis and the non-linear behaviour, with the determination of the limit cycle amplitudes, of a system with a non-linear rotor/stator contact are presented. The centre manifold theory and the rational approximants allow the reduction of the number of equations of the original system and the simplification of the non-linear terms in order to obtain a simplified system, without losing the dynamics of the original system, as well as the contributions of the non-linear terms. One of the advantages of the rational approximants is that they appear very interesting in regard to computational time; they also necessitate very few computer resources.

This procedure of using successively the centre manifold approach, the rational polynomial approximants, and the alternating frequency/time domain method is applicable for n-dimensional

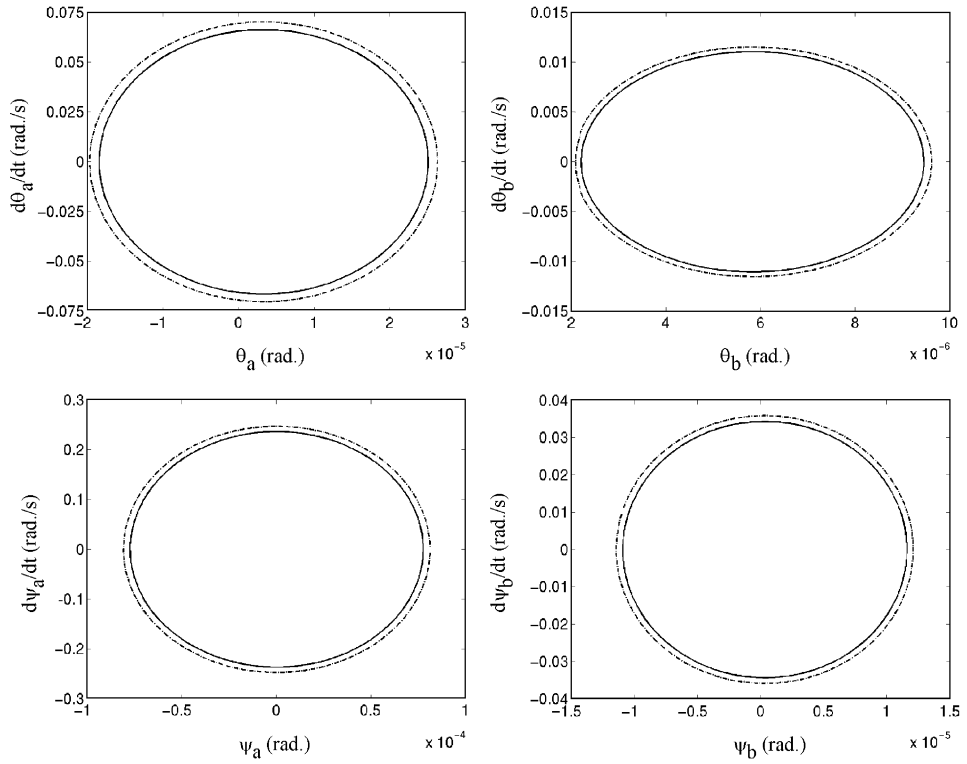

Fig. 20. θ_a, θ_b, ψ_a and ψ_b-limit cycles by using the centre manifold, the rational approximants and the alternating frequency/time method ($\mu = 1.1\mu_0$); — original system, - · - non-linear mathods.

Table 2
Values of the friction coefficient at the Hopf bifurcation point

Pressure (bar)	Friction coefficient μ_0 at the Hopf bifurcation point
10	0.41
15	0.33
20	0.47

systems with polynomial non-linearities. An application of these combined non-linear methods is proposed for a complex non-linear system with many degrees of freedom. The results from these non-linear methods are compared with those obtained by integrating the full original system. Excellent agreements are found between the original and the reduced system. Moreover, the methods require few computer resources and appear to be particularly interesting in the cases of large non-linear systems.

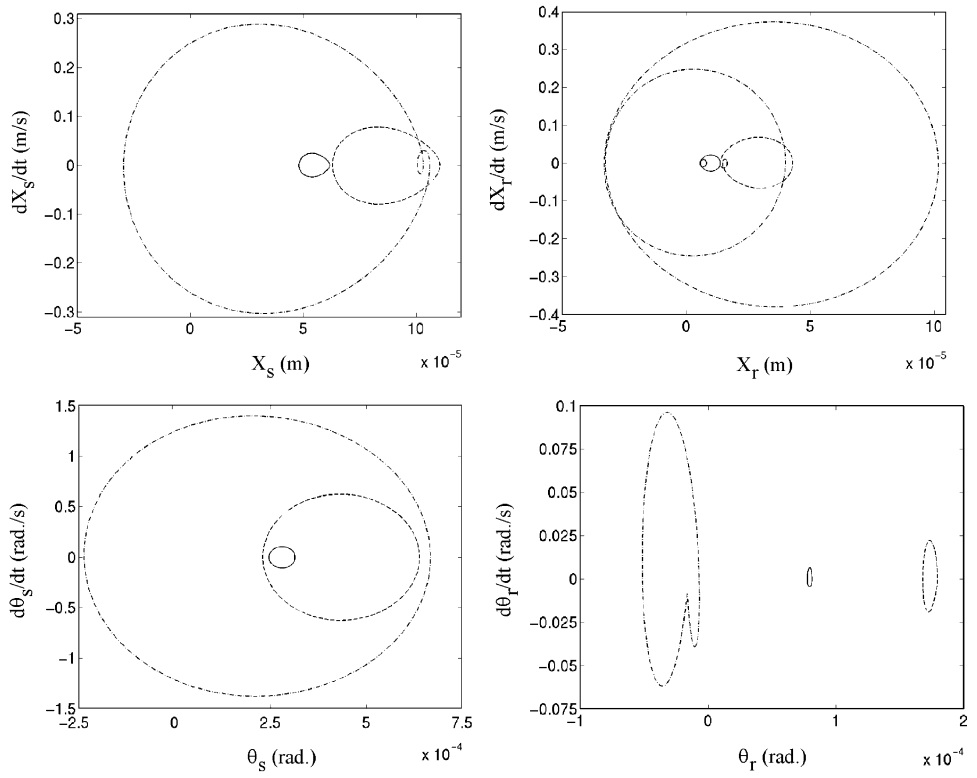

Fig. 21. Parametric studies for the X_s, X_r, θ_s and θ_r-limit cycles amplitudes ($\mu = 1.1\mu_0$); — $P_{hydraulic}$ =10 bars, - - - $P_{hydraulic}$ =15 bars, - - - $P_{hydraulic}$ = 20 bars.

Acknowledgements

The authors gratefully acknowledge the French Education Ministry for its support through Grant No. 99071 for the investigation presented here.

Appendix A. Equations of motion for the non-linear rotor/stator contact system

The equations of motion for the non-linear rotor/stator contact system are

$$m_s\ddot{x}_s + C_{xs}\dot{x}_s = F_{couple/X} + F_{hyd/X} - F_X, \tag{A.1}$$

$$I_{\theta s}\ddot{\theta}_s + C_{as}(\dot{\theta}_s - \dot{\theta}_a) + K_{\theta s}\theta_s + K_{as}(\theta_s - \theta_a) = F_{couple/X}R_e + F_{couple/Z}d_e + M_Y, \tag{A.2}$$

$$I_{\psi s}\ddot{\psi}_s + C_{as}(\dot{\psi}_s - \dot{\psi}_a) + K_{\psi s}\psi_s + K_{as}(\psi_s - \psi_a) = F_{couple/Y}d_e + M_Z, \tag{A.3}$$

$$I_{\varphi s}\ddot{\varphi}_s + C_{\varphi s}\dot{\varphi}_s = -F_{couple/Y}R_e + M_X, \tag{A.4}$$

$$m_r\ddot{x}_r + C_{xr}\dot{x}_r + K_{rr}x_r = F_X, \tag{A.5}$$

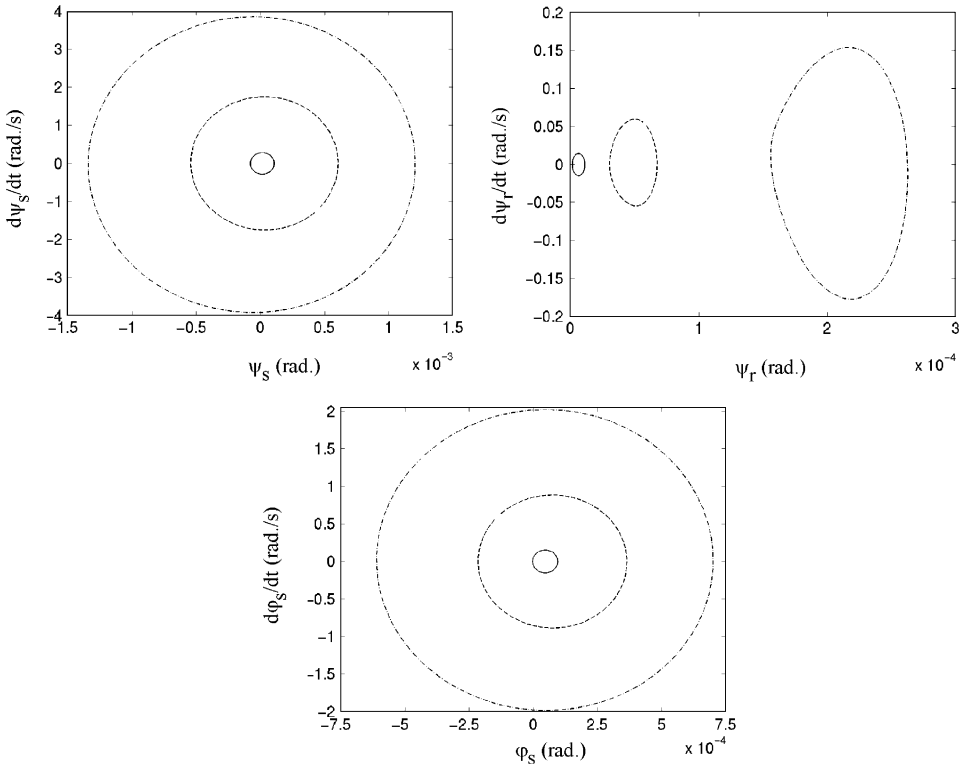

Fig. 22. Parametric studies for the ψ_s, ψ_r and φ_s-limit cycles amplitudes ($\mu = 1.1\mu_0$); — $P_{hydraulic}$ =10 bars, - - - $P_{hydraulic}$ =15 bars, - - - $P_{hydraulic}$ =20 bars.

$$I_{\theta r}\ddot{\theta}_r + C_{br}(\dot{\theta}_r - \dot{\theta}_b) + K_{br}(\theta_r - \theta_b) = -M_Y, \tag{A.6}$$

$$I_{\psi r}\ddot{\psi}_r + C_{br}(\dot{\psi}_r - \dot{\psi}_b) + K_{br}(\psi_r - \psi_b) = -M_Z, \tag{A.7}$$

$$m_b\ddot{y}_b + C_{b11}\dot{y}_b + C_{yab}(\dot{y}_b - \dot{y}_a) + K_{b11}y_b + K_{b12}\theta_b + K_{yab}(y_b - y_a) = 0, \tag{A.8}$$

$$I_b\ddot{\theta}_b + C_{b22}\dot{\theta}_b + C_{br}(\dot{\theta}_b - \dot{\theta}_r) + C_{\theta ab}(\dot{\theta}_b - \dot{\theta}_a) + K_{b21}y_b + K_{b22}\theta_b + K_{br}(\theta_b - \theta_r) + K_{\theta ab}(\theta_b - \theta_a) = 0, \tag{A.9}$$

$$m_b\ddot{z}_b + C_{b11}\dot{z}_b + C_{zab}(\dot{z}_b - \dot{z}_a) + K_{b11}z_b + K_{b12}\psi_b + K_{zab}(z_b - z_a) = 0, \tag{A.10}$$

$$I_b\ddot{\psi}_b + C_{b22}\dot{\psi}_b + C_{br}(\dot{\psi}_b - \dot{\psi}_r) + C_{\psi ab}(\dot{\psi}_b - \dot{\psi}_a) + K_{b21}z_b + K_{b22}\psi_b + K_{br}(\psi_b - \psi_r) + K_{\psi ab}(\psi_b - \psi_a) = 0, \tag{A.11}$$

$$m_a\ddot{y}_a + C_{a11}\dot{y}_a + C_{yab}(\dot{y}_a - \dot{y}_b) + K_{a11}y_a + K_{a12}\theta_a + K_{yab}(y_a - y_b) = 0, \tag{A.12}$$

$$I_a\ddot{\theta}_a + C_{a22}\dot{\theta}_a + C_{as}(\dot{\theta}_a - \dot{\theta}_s) + C_{\theta ab}(\dot{\theta}_a - \dot{\theta}_b) + K_{a21}y_a + K_{a22}\theta_a + K_{as}(\theta_a - \theta_s) + K_{\theta ab}(\theta_a - \theta_b) = 0, \tag{A.13}$$

$$m_a\ddot{z}_a + C_{a11}\dot{z}_a + C_{zab}(\dot{z}_a - \dot{z}_b) + K_{a11}z_a + K_{a12}\psi_a + K_{zab}(z_a - z_b) = 0, \tag{A.14}$$

$$I_a\ddot{\psi}_a + C_{a22}\dot{\psi}_a + C_{as}(\dot{\psi}_a - \dot{\psi}_s) + C_{\psi ab}(\dot{\psi}_a - \dot{\psi}_b) + K_{a21}z_a + K_{a22}\psi_a + K_{as}(\psi_a - \psi_s) + K_{\psi ab}(\psi_a - \psi_b) = 0, \tag{A.15}$$

where x_s, x_r, θ_s, θ_r, ψ_s, ψ_r, φ_s, y_a, z_a, θ_a, ψ_a, y_b, z_b, θ_b and ψ_b are the stator and the rotor lateral displacement, the stator and rotor rotations, the piston torsional rotation and the axle deflections and rotations of the stator and rotor shaft, respectively. The stator and the shaft of the stator interact via notches on the inner perimeter of the disk. The rotor and the shaft of the rotor interact via drive keys on the outside of the disk. K_{as} and C_{as} define the stiffness and the damping between the stator and the shaft of the stator, called torque tube, via notches on the inner perimeter of the disk. K_{br} and C_{br} define the stiffness and the damping between the rotor and the shaft of the rotor, via drive keys on the outside of the disk. $K_{\psi ab}$, $K_{\theta ab}$, K_{yab}, K_{zab} and $C_{\psi ab}$, $C_{\theta ab}$, C_{yab}, C_{zab} represent the contact stiffness and the contact damping between the rotor's and stator's shaft, respectively. K_{rr} represents the stiffness of the backplate of the brake. K_{aij} $(i, j = 1, 2)$ and C_{aij} $(i, j = 1, 2)$ are the axle bend stiffness and axle bend damping for the stator's shaft, respectively. K_{bij} $(i, j = 1, 2)$ and C_{bij} $(i, j = 1, 2)$ are the axle bend stiffness and axle bend damping for the rotor's shaft, respectively. d_e and R_e represent the brake rod lateral offset and the distance axle to brake rod axis. F_X, M_X, M_Y and M_Z are the normal contact between the rotor and the stator friction surfaces and the associated moments, respectively. These expressions are given in Eqs. (9)–(12). $F_{couple/X}$, $F_{couple/Y}$ and $F_{couple/Z}$ represent the load due to the brake rod. One has

$$\begin{aligned} F_{couple/X} &= K_{rod}R_e\phi_s \sin\alpha + K_{rod}x_s \sin\alpha + K_{rod}R_e\theta_s \sin\alpha, \\ F_{couple/Y} &= K_{rod}R_e\phi_s \cos\alpha - K_{rod}d_e\theta_s \cos\alpha, \\ F_{couple/Z} &= K_{rod}R_e\phi_s \cos\alpha - K_{rod}d_e\psi_s \cos\alpha, \end{aligned} \tag{A.16}$$

where K_{rod} defines the axial stiffness of the brake rod and α the sprag-slip angle due to the brake rod angle offset with the rotor/stator interface.

$F_{hyd/X}$ is the brake force due to the hydraulic pressure. It is given by

$$F_{hyd/X} = P_{hydraulic}n_{piston}\frac{(R^2_{piston/outer} - R^2_{piston/inner})}{(R_0^2 - R_i^2)}, \tag{A.17}$$

where n_{piston}, $R_{piston/outer}$, $R_{piston/inner}$ are the number of pistons, the outer and inner radius of the piston surface in contact with the stator, respectively. R_0 and R_i define the outer and inner radius of the rotor/stator interface, respectively.

The vector $\mathbf{F}_{contact}$ defines the linear and non-linear rotor/stator friction contact. It is given by

$$\mathbf{F}_{contact}(1) = -\mathbf{F}_{contact}(5) = -F_X, \tag{A.18}$$

$$\mathbf{F}_{contact}(2) = -\mathbf{F}_{contact}(6) = -M_Y, \tag{A.19}$$

$$\mathbf{F}_{contact}(3) = -\mathbf{F}_{contact}(7) = -M_Z, \tag{A.20}$$

$$\mathbf{F}_{contact}(4) = M_X, \tag{A.21}$$

$$\mathbf{F}_{contact}(i) = 0 \quad \text{for } 8 \leqslant i \leqslant 15. \tag{A.22}$$

The vector $\mathbf{F}$ defines the hydraulic brake command. It is given by

$$\mathbf{F}(1) = -\mathbf{F}_{hydraulic}, \tag{A.23}$$

$$\mathbf{F}_{contact}(i) = 0 \quad \text{for } 2 \leqslant i \leqslant 15. \tag{A.24}$$

The vector $\mathbf{F}_{couple}$ defines the hydraulic brake command. It is given by

$$\mathbf{F}_{couple}(1) = F_{couple/X}, \tag{A.25}$$

$$\mathbf{F}_{couple}(2) = F_{couple/Z} d_e, \tag{A.26}$$

$$\mathbf{F}_{couple}(3) = F_{couple/Y} d_e, \tag{A.27}$$

$$\mathbf{F}_{couple}(4) = -F_{couple/Y} R_e, \tag{A.28}$$

$$\mathbf{F}_{contact}(i) = 0 \quad \text{for } 5 \leqslant i \leqslant 15. \tag{A.29}$$

This non-linear 15-degree-of-freedom system has the form

$$\mathbf{M}\ddot{\mathbf{x}} + \mathbf{C}\dot{\mathbf{x}} + \mathbf{K}\mathbf{x} = \mathbf{F} + \mathbf{F}_{couple}(\mathbf{x}) + \mathbf{F}_{contact}(\mathbf{x}), \tag{A.30}$$

where $\ddot{\mathbf{x}}$, $\dot{\mathbf{x}}$ and $\mathbf{x}$ are the acceleration, velocity, and displacement response 15-dimensional vectors of the degrees of freedom, respectively. $\mathbf{M}$ is the mass matrix, $\mathbf{C}$ is the damping matrix and $\mathbf{K}$ is the stiffness matrix. $\mathbf{F}$ is the vector force due to net brake hydraulic pressure. $\mathbf{F}_{contact}$ contains the linear and non-linear contact force terms at the stator and rotor interface and $\mathbf{F}_{couple}$ define the brake rod load, respectively. Finally, the general form of the equation of motion for the non-linear system can be expressed in the following way:

$$\mathbf{M}\ddot{\mathbf{x}} + \mathbf{C}\dot{\mathbf{x}} + \hat{\mathbf{K}}\mathbf{x} = \mathbf{F} + \mathbf{F}_{contact}(\mathbf{x}) \tag{A.31}$$

with

$$\mathbf{F}_{couple}(\mathbf{x}) = \hat{\mathbf{K}}\mathbf{x}. \tag{A.32}$$

Appendix B. Brake parameters

R_0	outer radius of the rotor/stator interface (= 0.076 m)
R_i	inner radius of the rotor/stator interface (= 0.024 m)
n_{piston}	number of pistons (= 6)
$R_{piston/outer}$	outer radius of the piston surface in contact with the stator (= 0.015 m)
$R_{piston/inner}$	inner radius of the piston surface in contact with the stator (= 0.0075 m)
d_e	brake rod lateral offset (= 0.01 m)
R_e	distance axle to brake rod axis (= 0.064 m)
K_1	linear coefficient of the non-linear rotor/stator contact ($= 4.6 \times 10^8$ N/m^3)
K_2	quadratic coefficient of the non-linear rotor/stator contact ($= 4.8 \times 10^{11}$ N/m^4)
K_3	cubic coefficient of the non-linear rotor/stator contact ($= 9.5 \times 10^{16}$ N/m^5)
m_s	mass of the stator (= 5 kg)

m_r mass of the rotor (= 5 kg)
$I_{\theta r} = I_{\psi r}$ moments of inertia for the rotor (= 0.35 kg m^2)
$I_{\theta s} = I_{\psi s}$ moments of inertia for the stator (= 0.28 kg m^2)
$I_{\varphi s}$ φ-moment of inertia for the stator (= 0.35 kg m^2)
m_a equivalent mass of the stator shaft (= 67.5 kg)
m_b equivalent mass of the rotor shaft (= 185 kg)
I_a axle moment of inertia for the stator shaft (= 1.2 kg m^2)
I_b axle moment of inertia for the rotor shaft (= 0.7 kg m^2)
$P_{hydraulic}$ net brake hydraulic pressure (= 10 bars)
$K_{\theta s}$ stator θ-stiffness (= 2.25×10^6 N m/rad)
$K_{\psi s}$ stator ψ-stiffness (= 2.25×10^6 N m/rad)
$K_{\varphi s}$ stator torsional stiffness (= 2.8×10^7 N m/rad)
$C_{\varphi s}$ stator torsional damping (= 15 N m s/rad)
K_{as} lateral stiffness between the stator and the shaft of the stator (= 3.3×10^8 N m/rad)
K_{rr} stiffness between the rotor and the backplate of the brake (= 1.2×10^7 N/m)
C_{xs} lateral damping coefficient for the stator (= 60 N/m s)
C_{xr} lateral damping coefficient for the rotor (= 120 N/m s)
C_{as} damping between the stator and the shaft of the stator (= 1200 N/m s)
K_{br} lateral stiffness between the rotor and the shaft of the rotor (= 3.3×10^8 N m/rad)
C_{br} damping between the rotor and the shaft of the rotor (= 1500 N/m s)
$K_{\psi ab}$ ψ-stiffness between the rotor and stator shaft (= 4.5×10^6 N m/rad)
$K_{\theta ab}$ θ-stiffness between the rotor and stator shaft (= 4.5×10^6 N m/rad)
K_{yab} y-lateral stiffness between the rotor and stator shaft (= 3.25×10^8 N/m)
K_{zab} z-lateral stiffness between the rotor and stator shaft (= 3.25×10^8 N/m)
$C_{\psi ab} = C_{\theta ab}$ rotational damping between the rotor and stator shaft (= 1 N m s/rad)
$C_{yab} = C_{zab}$ lateral damping between the rotor and stator shaft (= 1500 N/m s)
K_{a11} y–y stiffness and z–z stiffness of the stator shaft (= 1.8×10^9 N/m)
K_{a12} y–θ stiffness and z–ψ stiffness of the stator shaft (= 2.1×10^8 N/rad)
K_{a22} θ–θ stiffness and ψ–ψ stiffness of the stator shaft (= 4.3×10^7 N m/rad)
K_{b11} y–y stiffness and z–z stiffness of the rotor shaft (= 8.9×10^7 N/m)
K_{b12} y–θ stiffness and z–ψ stiffness of the rotor shaft (= 2.5×10^7 N/rad)
K_{b22} θ–θ stiffness and ψ–ψ stiffness of the rotor shaft (= 9.6×10^6 N m/rad)
C_{a11} y–y damping and z–z damping of the stator shaft (= 6900 N/m s)
C_{a22} θ–θ damping and ψ–ψ damping of the stator shaft (= 2 N m s/rad)
C_{b11} y–y damping and z–z damping of the rotor shaft (= 6900 N/m s)
C_{b22} θ–θ damping and ψ–ψ damping of the rotor shaft (= 2 N m s/rad)
α sprag-slip angle (= 0.005 rad)

Appendix C. Analytical expression of the coefficients $a_{k,ijl}$ for the second and third orders

One determines the analytical expressions of $\mathbf{h}$ as a power series in $(\mathbf{v}_c, \hat{\mu})$ of degree 3, for a n-dimensional differential equations with quadratic and cubic non-linear terms ($n = 30$ in this study).

The developed expression of Eq. (46) has the form

$$\dot{\mathbf{v}}_c = \mathbf{J}_c\mathbf{v}_c + \mathbf{G}_2(\mathbf{v}) + \mathbf{G}_3(\mathbf{v}) = \mathbf{J}_c\mathbf{v}_c + G^{ij}_{(2)}\mathbf{v}\otimes\mathbf{v} + G^{ik}_{(3)}\mathbf{v}\otimes\mathbf{v}\otimes\mathbf{v},$$

$$\dot{\mathbf{v}}_s = \mathbf{J}_s\mathbf{v}_s + \mathbf{H}_2(\mathbf{v}) + \mathbf{H}_3(\mathbf{v}) = \mathbf{J}_s\mathbf{v}_s + H^{ij}_{(2)}\mathbf{v}\otimes\mathbf{v} + H^{ik}_{(3)}\mathbf{v}\otimes\mathbf{v}\otimes\mathbf{v},$$

$$\dot{\hat{\mu}} = 0 \tag{C.1}$$

with $\mathbf{v} = \{\mathbf{v}_c^{\mathrm{T}}\ \mathbf{v}_s^{\mathrm{T}}\ \hat{\mu}\}^{\mathrm{T}}$. $G^{ij}_{(2)}$, $G^{ik}_{(3)}$, $H^{ij}_{(2)}$ and $H^{ik}_{(3)}$ are quadratic and cubic non-linear terms of $\mathbf{v}$, respectively (with $i = 1, 2$, $1 \leqslant l \leqslant n-2$, $1 \leqslant j \leqslant (n+1)^2$ and $1 \leqslant k \leqslant (n+1)^3$). $\otimes$ defines the Kronecker product. These notations will be used to define expressions for the coefficients of the polynomial approximations $\mathbf{v}_s = \mathbf{h}(\mathbf{v}_c, \hat{\mu})$ as a power series in $(\mathbf{v}_c, \hat{\mu})$.

Firstly, one can express the stable variables by using second order polynomial approximations. One recalls that the polynomial approximations contain no constant and linear terms. So, the expressions of the stable variables $\mathbf{v}_s$ as a power series in $(\mathbf{v}_c, \hat{\mu})$ of degree 2 can be written as

$$\begin{aligned}\mathbf{v}_s = \mathbf{h}^{(1)}(\mathbf{v}_c, \hat{\mu}) = \mathbf{h}^{(1)}(v_{c1}, v_{c2}, \hat{\mu}) &= \sum_{p=i+j+l=2}^{2}\ \sum_{j=0}^{p}\ \sum_{l=0}^{p} \mathbf{a}_{ijl} v_{c1}^i v_{c2}^j \hat{\mu}^l \\ &= \mathbf{a}_{200}v_{c1}^2 + \mathbf{a}_{110}v_{c1}v_{c2} + \mathbf{a}_{020}v_{c2}^2 + \mathbf{a}_{101}v_{c1}\hat{\mu} + \mathbf{a}_{011}v_{c2}\hat{\mu} + \mathbf{a}_{002}\hat{\mu}^2,\end{aligned} \tag{C.2}$$

where $\mathbf{a}_{ijl}$ are unknown vectors of coefficients. The analytical expression of $\mathbf{a}_{ijl}$ can be determined by equating (47), and by considering only second-order terms. The simplified expression of Eq. (47) has the form

$$D_{v_c,\hat{\mu}}(\mathbf{h}^{(1)}(\mathbf{v}_c, \hat{\mu}))\mathbf{J}_c\mathbf{v}_c - \mathbf{J}_s\mathbf{h}^{(1)}(\mathbf{v}_c, \hat{\mu}) - \mathbf{H}_2(\mathbf{v}_c, \hat{\mu}) = 0. \tag{C.3}$$

One notes that this system is the exact system for second-order polynomial approximations. It is possible to obtain an analytical expression of the coefficients $a_{k,ijl}$ by solving Eq. (C.3). One obtains

$$a_{k,200} = \frac{H^{k,1}_{(2)}}{(2J_{c1} - J_{sk})},$$

$$a_{k,110} = \frac{H^{k,2}_{(2)} + H^{k,n+2}_{(2)}}{(J_{c1} + J_{c2} - J_{sk})},$$

$$a_{k,020} = \frac{H^{k,n+3}_{(2)}}{(2J_{c2} - J_{sk})},$$

$$a_{k,101} = \frac{H^{k,n+1}_{(2)} + H^{k,n(n+1)+1}_{(2)}}{(J_{c1} - J_{sk})},$$

$$a_{k,011} = \frac{H^{k,2(n+1)}_{(2)} + H^{k,n(n+1)+2}_{(2)}}{(J_{c2} - J_{sk})},$$

$$a_{k,002} = \frac{-H^{k,(n+1)^2}_{(2)}}{J_{sk}},$$

where k defines the kth degree of freedom of stable variables ($1 \leqslant k \leqslant n-2$). J_{c1} and J_{c2} are the first and second terms of the diagonal matrix $\mathbf{J}_c$ as defined in Eq. (C.1), respectively. J_{sk} is the kth term of the diagonal matrix $\mathbf{J}_s$. $H_{(2)}^{k,i}$ defined the term of the kth line and ith column of the matrix defined by $\mathbf{H}_2$.

If the second order approximation is not sufficient, it is necessary to define the third-polynomial approximation in order to describe correctly the dynamics of the system. Then, the expressions of the stable variables $\mathbf{v}_s$, as a power series in $(\mathbf{v}_c, \hat{\mu})$ of degree, can be defined by adding third order polynomial terms in the first second order polynomial approximation defined in Eq. (C.2). These expressions have the form

$$\begin{aligned}\mathbf{v}_s &= \sum_{p=i+j+l=2}^{3} \sum_{j=0}^{p} \sum_{l=0}^{p} \mathbf{a}_{ijl} v_{c1}^{i} v_{c2}^{j} \hat{\mu}^{l} = \mathbf{h}^{(1)}(\mathbf{v}_c, \hat{\mu}) + \mathbf{h}^{(2)}(\mathbf{v}_c, \hat{\mu}) \\ &= \mathbf{h}^{(1)}(\mathbf{v}_c, \hat{\mu}) + \mathbf{a}_{300} v_{c1}^{3} + \mathbf{a}_{210} v_{c1}^{2} v_{c2} + \mathbf{a}_{120} v_{c1} v_{c2}^{2} + \mathbf{a}_{030} v_{c2}^{3} \\ &\quad + \mathbf{a}_{201} v_{c1}^{2} \hat{\mu} + \mathbf{a}_{111} v_{c1} v_{c2} \hat{\mu} + \mathbf{a}_{021} v_{c2}^{2} \hat{\mu} + \mathbf{a}_{102} v_{c1} \hat{\mu}^{2} + \mathbf{a}_{012} v_{c2} \hat{\mu}^{2} + \mathbf{a}_{003} \hat{\mu}^{3}, \end{aligned} \tag{C.4}$$

where $\mathbf{a}_{ijl}$ are unknown vectors of coefficients (for $i+j+l=3$). $\mathbf{h}^{(1)}(\mathbf{v}_c, \hat{\mu})$ defines the first approximation using second order polynomial approximation.

It is possible to obtain an analytical expression of the coefficients $a_{k,ijl}$ by solving the simplified expression of Eq. (47)

$$\begin{aligned} &D_{v_c,\hat{\mu}}(\mathbf{h}^{(1)}(\mathbf{v}_c, \hat{\mu}))[\mathbf{G}_2(\mathbf{v}_c, \hat{\mu})] + D_{v_c}(\mathbf{h}^{(2)}(\mathbf{v}_c, \hat{\mu}))\mathbf{J}_c\mathbf{v}_c \\ &- \mathbf{J}_s\mathbf{v}_s - \mathbf{H}_2(\{\mathbf{v}_c, \mathbf{0}, \hat{\mu}\} \otimes \{\mathbf{v}_c, \mathbf{h}^{(1)}(\mathbf{v}_c, \hat{\mu}), \hat{\mu}\} - \{\mathbf{0}, \mathbf{h}^{(1)}(\mathbf{v}_c, \hat{\mu}), 0\} \otimes \{\mathbf{v}_c, \mathbf{0}, \hat{\mu}\}) - \mathbf{H}_3(\mathbf{v}_c, \hat{\mu}) = 0. \end{aligned} \tag{C.5}$$

One obtains

$$a_{k,300} = \frac{-2a_{k,200}G_{(2)}^{1,1} - a_{k,110}G_{(2)}^{2,1} + H_{(3)}^{k,1} + \sum_{i=1}^{n-2} a_{i,200}(H_{(2)}^{k,2+i} + H_{(2)}^{k,(n+1)(i+1)+1})}{3J_{c1} - J_{sk}},$$

$$a_{k,210} = \frac{\begin{pmatrix} -2a_{k,200}(G_{(2)}^{1,2} + G_{(2)}^{1,n+2}) - a_{k,110}(G_{(2)}^{1,1} + G_{(2)}^{2,2} + G_{(2)}^{2,n+2}) - 2a_{k,020}G_{(2)}^{2,1} + H_{(3)}^{k,2} + H_{(3)}^{k,n+2} \\ + H_{(3)}^{k,(n+1)^2+1} + \sum_{i=1}^{n-2} a_{i,110}(H_{(2)}^{k,i+2} + H_{(2)}^{k,(n+1)(i+1)+1}) + \sum_{i=1}^{n-2} a_{i,200}(H_{(2)}^{k,n+i+3} + H_{(2)}^{k,(n+1)(i+1)+2}) \end{pmatrix}}{2J_{c1} + J_{c2} - J_{sk}},$$

$$a_{k,120} = \frac{\begin{pmatrix} -2a_{k,020}(G_{(2)}^{2,2} + G_{(2)}^{2,n+2}) - a_{k,110}(G_{(2)}^{2,n+3} + G_{(2)}^{1,2} + G_{(2)}^{1,n+2}) - 2a_{k,200}G_{(2)}^{1,n+3} + H_{(3)}^{k,n+3} + H_{(3)}^{k,(n+1)^2+2} \\ + H_{(3)}^{k,(n+1)^2+n+2} + \sum_{i=1}^{n-2} a_{i,020}(H_{(2)}^{k,i+2} + H_{(2)}^{k,(n+1)(i+1)+1}) + \sum_{i=1}^{n-2} a_{i,110}(H_{(2)}^{k,n+i+2} + H_{(2)}^{k,(n+1)(i+1)+2}) \end{pmatrix}}{J_{c1} + 2J_{c2} - J_{sk}},$$

$$a_{k,030} = \frac{-2a_{k,020}G_{(2)}^{2,n+3} - a_{k,110}G_{(2)}^{1,n+3} + H_{(3)}^{k,(n+1)^2+n+2} + \sum_{i=1}^{n-2} a_{i,020}(H_{(2)}^{k,n+i+3} + H_{(2)}^{k,(n+1)(i+1)+2})}{3J_{c2} - J_{sk}},$$

$$a_{k,201}=\frac{\left(\begin{array}{l}-a_{k,101}G_{(2)}^{1,1}-a_{k,011}G_{(2)}^{2,1}-2a_{k,200}(G_{(2)}^{1,n+1}+G_{(2)}^{1,n(n+1)+1})-a_{k,110}(G_{(2)}^{2,n+1}+G_{(2)}^{2,n(n+1)+1})\\+H_{(3)}^{k,n(n+1)+1}+H_{(3)}^{k,n+1}+H_{(3)}^{k,n(n+1)^2+1}+\sum_{i=1}^{n-2}a_{i,101}(H_{(2)}^{k,i+1}+H_{(2)}^{k,(n+1)(i+1)+1})\\+\sum_{i=1}^{n-2}a_{i,200}(H_{(2)}^{k,(n+1)(2+i)}+H_{(2)}^{k,n(n+1)+i+2})\end{array}\right)}{2J_{c1}-J_{sk}},$$

$$a_{k,021}=\frac{\left(\begin{array}{l}-a_{k,101}G_{(2)}^{1,n+3}-a_{k,011}G_{(2)}^{2,n+3}-2a_{k,020}(G_{(2)}^{2,2(n+1)}+G_{(2)}^{2,n(n+1)+2})-a_{k,110}(G_{(2)}^{1,2(n+1)}+G_{(2)}^{1,n(n+1)+2})\\+H_{(3)}^{k,(n+1)^3-2(2n+1)}+\sum_{i=1}^{n-2}a_{i,020}(H_{(2)}^{k,(n+1)(2+i)}+H_{(2)}^{k,n(n+1)+i+2})\\+\sum_{i=1}^{n-2}a_{i,011}(H_{(2)}^{k,2n-1+i}+H_{(2)}^{k,(n+1)(i+1)+2})+H_{(3)}^{k,(n+1)^2+2(n+1)}+H_{(3)}^{k,2(n+1)^2-n+1}\end{array}\right)}{2J_{c2}-J_{sk}},$$

$$a_{k,102}=\frac{\left(\begin{array}{l}-2a_{k,200}G_{(2)}^{1,(n+1)^2}-a_{k,110}G_{(2)}^{2,(n+1)^2}-a_{k,101}(G_{(2)}^{1,n+1}+G_{(2)}^{1,n(n+1)+1})-a_{k,011}(G_{(2)}^{2,n+1}+G_{(2)}^{2,(n+1)n+1})\\+H_{(3)}^{k,(n+1)^3-n}+\sum_{i=1}^{n-2}a_{i,101}(H_{(2)}^{k,(n+1)(2+i)}+H_{(2)}^{k,(n+1)n+i+2})+\sum_{i=1}^{n-2}a_{i,002}(H_{(2)}^{k,i+2}+H_{(2)}^{k,(n+1)(i+1)+1})\\+H_{(3)}^{k,(n+1)^2}+H_{(3)}^{k,n(n+1)^2+n+1}\end{array}\right)}{J_{c1}-J_{sk}},$$

$$a_{k,012}=\frac{\left(\begin{array}{l}-a_{k,110}G_{(2)}^{1,(n+1)^2}-2a_{k,020}G_{(2)}^{2,(n+1)^2}-a_{k,101}(G_{(2)}^{1,2(n+1)}+G_{(2)}^{1,n(n+1)+2})-a_{k,011}(G_{(2)}^{2,2(n+1)}+G_{(2)}^{2,n(n+1)+2})\\+H_{(3)}^{k,2(n+1)^2}+\sum_{i=1}^{n-2}a_{i,011}(H_{(2)}^{k,(n+1)(2+i)}+H_{(2)}^{k,n(n+1)+i+2})+\sum_{i=1}^{n-2}a_{i,002}(H_{(2)}^{k,2n-1+i}+H_{(2)}^{k,(n+1)(i+1)+2})\\+H_{(3)}^{k,n(n+1)^2+2(n+1)}+H_{(3)}^{k,(n+1)^3-n+1}\end{array}\right)}{J_{c2}-J_{sk}},$$

$$a_{k,111}=\frac{\left(\begin{array}{l}-a_{k,101}(G_{(2)}^{1,2}+G_{(2)}^{1,n+2})-a_{k,110}(G_{(2)}^{1,n+1}+G_{(2)}^{1,n(n+1)+1}+G_{(2)}^{1,2(n+1)}+G_{(2)}^{1,n(n+1)+2})\\-2a_{k,200}(G_{(2)}^{1,2(n+1)}+G_{(2)}^{1,n(n+1)+2})+H_{(3)}^{k,n(n+1)+2}-2a_{k,020}(G_{(2)}^{2,n+1}+G_{(2)}^{2,n(n+1)+1})-a_{k,011}(G_{(2)}^{2,2}+G_{(2)}^{2,n+2})\\+H_{(3)}^{k,2(n+1)}+H_{(3)}^{k,2(n+1)^2-n}+H_{(3)}^{k,(n+1)^2+n+1}+H_{(3)}^{k,n(n+1)^2+n-2}+H_{(3)}^{k,n(n+1)^2+n+2}\\+\sum_{i=1}^{n-2}a_{i,110}(H_{(2)}^{k,(n+1)(i+2)}+H_{(2)}^{k,n(n+1)+i+2})+\sum_{i=1}^{n-2}a_{i,101}(H_{(2)}^{k,2n-1+i}+H_{(2)}^{k,(n+1)(i+1)+2})\\+\sum_{i=1}^{n-2}a_{i,011}(H_{(2)}^{k,i+2}+H_{(2)}^{k,(n+1)(i+1)+1})\end{array}\right)}{J_{c1}+J_{c2}-J_{sk}},$$

$$a_{k,003}=\frac{a_{k,102}G_{(2)}^{1,(n+1)^2}+a_{k,012}G_{(2)}^{2,(n+1)^2}-H_{(3)}^{k,(n+1)^3}-\sum_{i=1}^{n-2}a_{i,002}(H_{(2)}^{k,(n+1)(2+i)}+H_{(2)}^{k,n(n+1)+i+2})}{J_{sk}},$$

where k defines the kth degree of freedom of stable variables. J_{c1} and J_{c2} are the first and second terms of the diagonal matrix $\mathbf{J}_c$. J_{sk} is the kth term of the diagonal matrix $\mathbf{J}_s$. $H_{(2)}^{ki}$ and $H_{(3)}^{ki}$ defined the terms of the kth line and ith column of the matrix defined by $\mathbf{H}_2$ and $\mathbf{H}_3$, respectively. $G_{(2)}^{ki}$ defined the term of the kth line and ith column of the matrix defined by $\mathbf{G}_2$.

Appendix D. Definition of the terms for the AFT method

The k-incremental vector of Fourier coefficients are arranged as follows:

$$\mathbf{V}^k = \{\{\mathbf{V}_0^k\}^{\mathrm{T}}, \ldots, \{\mathbf{V}_{2j-1}^k\}^{\mathrm{T}}, \{\mathbf{V}_{2j}^k\}^{\mathrm{T}}, \ldots, \{\mathbf{V}_{2H}^k\}^{\mathrm{T}}\}^{\mathrm{T}}.$$

The Jacobian matrices $\mathbf{A}$ and $\mathbf{J}$ are given by

$$\mathbf{A} = \begin{bmatrix} \mathbf{O} & & & & & & \\ & \mathbf{A}^{(1)} & & & & & \\ & & \ddots & & & & \\ & & & \mathbf{A}^{(j)} & & & \\ & & & & \ddots & & \\ & & & & & \mathbf{A}^{(H)} & \end{bmatrix}$$

and

$$\mathbf{J} = (\Gamma \otimes \mathbf{I}) \begin{bmatrix} \ddots & & & \\ & \dfrac{\partial f_1^{NL}}{\partial v_{c1}} & \dfrac{\partial f_1^{NL}}{\partial v_{c2}} & \\ & \dfrac{\partial f_2^{NL}}{\partial v_{c1}} & \dfrac{\partial f_2^{NL}}{\partial v_{c2}} & \\ & & & \ddots \end{bmatrix} (\Gamma^{-1} \otimes \mathbf{I}),$$

where

$$\mathbf{A}^{(j)} = \begin{bmatrix} \mathbf{O} & j\omega\mathbf{I} \\ -j\omega\mathbf{I} & \mathbf{O} \end{bmatrix} \quad (\text{for } j = 1, \ldots, H), \quad \mathbf{I} = \begin{bmatrix} 1 & 0 \\ 0 & 1 \end{bmatrix} \text{ and } \mathbf{O} = \begin{bmatrix} 0 & 0 \\ 0 & 0 \end{bmatrix}.$$

By considering the expressions

$$f_\alpha^{NL}(x, y) = \frac{\sum_{(i,j)\in S_M} n_{\alpha.ij} v_{c1}^i v_{c2}^j}{\sum_{(i,j)\in S_N} d_{\alpha.ij} v_{c1}^i v_{c2}^j} \quad (\text{for } \alpha = 1, 2)$$

with $S_M = \{(i, j) \,|\, 0 \leqslant i \leqslant M,\ 0 \leqslant j \leqslant M\}$ and $S_N = \{(i, j) \,|\, 0 \leqslant i \leqslant N,\ 0 \leqslant j \leqslant N\}$, the expressions $\partial f_\alpha^{NL}/\partial v_{c1}$ and $\partial f_\alpha^{NL}/\partial v_{c2}$ (for $\alpha = 1, 2$) are given by

$$\frac{\partial f_\alpha^{NL}}{\partial v_{c1}} = \frac{i(\sum_{(i,j)\in S_M} n_{\alpha.ij} v_{c1}^{(i-1)} v_{c2}^j \times \sum_{(i,j)\in S_N} d_{\alpha.ij} v_{c1}^i v_{c2}^j - \sum_{(i,j)\in S_M} n_{\alpha.ij} v_{c1}^i v_{c2}^j \times \sum_{(i,j)\in S_N} d_{\alpha.ij} v_{c1}^{(i-1)} v_{c2}^j)}{(\sum_{(i,j)\in S_N} d_{\alpha.ij} v_{c1}^i v_{c2}^j)^2}$$

and

$$\frac{\partial f_\alpha^{NL}}{\partial v_{c2}} = \frac{j(\sum_{(i,j)\in S_M} n_{\alpha.ij} v_{c1}^i v_{c2}^{(j-1)} \times \sum_{(i,j)\in S_N} d_{\alpha.ij} v_{c1}^i v_{c2}^j - \sum_{(i,j)\in S_M} n_{\alpha.ij} v_{c1}^i v_{c2}^j \times \sum_{(i,j)\in S_N} d_{\alpha.ij} v_{c1}^i v_{c2}^{(j-1)})}{(\sum_{(i,j)\in S_N} d_{\alpha.ij} v_{c1}^i v_{c2}^j)^2}.$$

The DFT from time to frequency domain is given by

$$\Gamma_{ij} = \begin{cases} \dfrac{1}{2H+1} & \text{for } i = 1, \\ \dfrac{2}{2H+1}\cos\left(\dfrac{(j-1)i\pi}{2H+1}\right) & \text{for } i = 2,4,\ldots,2H \\ \dfrac{2}{2H+1}\sin\left(\dfrac{(j-1)(i-1)\pi}{2H+1}\right) & \text{for } i = 1,3,\ldots,2H+1 \end{cases} \qquad \text{for } j = 1,2,\ldots,2H+1,$$

and from frequency time domain:

$$\Gamma_{ij}^{-1} = \begin{cases} 1 & \text{for } j = 1, \\ \cos\left(\dfrac{(i-1)j\pi}{2H+1}\right) & \text{for } j = 2,4,\ldots,2H \\ \sin\left(\dfrac{(i-1)(j-1)\pi}{2H+1}\right) & \text{for } j = 1,3,\ldots,2H+1. \end{cases} \qquad \text{for } i = 1,2,\ldots,2H+1,$$

Appendix E. Nomenclature

x	scalar
$\mathbf{x}$	vector
$\dot{\mathbf{x}}$	vector of velocity
$\ddot{\mathbf{x}}$	vector of acceleration
$\mathbf{x}_0$	equilibrium point
$\bar{\mathbf{x}}$	small perturbation
$\mathbf{C}$	damping matrix
$\mathbf{K}$	stiffness matrix
$\mathbf{M}$	mass matrix
$\mathbf{F}$	vector force due to the net hydraulic pressure
$\mathbf{F}_{contact}$	vector of linear and non-linear terms due to the rotor/stator contact
$\mathbf{F}_{couple}$	vector of the brake rod load
$\mathbf{F}_{contact}^{L}$	vector of linear terms due to the rotor/stator contact
$\mathbf{F}_{contact}^{NL}$	vector of non-linear terms due to the rotor/stator contact
$\mathbf{a}_{ijl}$	vector of the coefficients of the centre manifold
$\mathbf{v}_c$	vector of centre variables
$\mathbf{v}_s$	vector of stable variables
$\mathbf{h}$	vector of the polynomial approximation of stable variables in centre variables
$\mathbf{J}_s$	Jacobian matrix of stable variables
$\mathbf{J}_c$	Jacobian matrix of centre variables
$\mathbf{G}$	vector function of quadratic and cubic terms for the centre variables
$\mathbf{H}$	vector function of quadratic and cubic terms for the stable variables
n_{ij}	coefficients of the denominator of the rational approximants
d_{ij}	coefficients of the numerator of the rational approximants

$\mathbf{V}_i$ vector of Fourier coefficients
x_s lateral displacement of the stator
x_r lateral displacement of the rotor
θ_s rotation of the stator
θ_r rotation of the rotor
ψ_s rotation of the stator
ψ_r rotation of the rotor
φ_s the axle deflections and rotations of the stator and rotor shaft
y_a axle deflection of the stator shaft
z_a axle deflection of the stator shaft
θ_a axle rotation of the stator shaft
ψ_a axle rotation of the stator shaft
y_b axle deflection of the rotor shaft
z_b axle deflection of the rotor shaft
θ_b axle rotation of the rotor shaft
ψ_b axle rotation of the rotor shaft
α sprag-slip angle
μ brake friction coefficient
μ_0 brake friction coefficient at the Hopf bifurcation point

References

[1] A.H. Nayfeh, B. Balachandran, *Applied Nonlinear Dynamics: Analytical, Computational and Experimental Methods*, Wiley, New York, 1995.
[2] A.D. Brjuno, Analytical forms of differential equations, I, *Transactions of the Moscow Mathematical Society* 25 (1971) 132–198.
[3] A.D. Brjuno, Analytical forms of differential equations, II, *Transactions of the Moscow Mathematical Society* 25 (1972) 199–299.
[4] J. Guckenheimer, P. Holmes, *Nonlinear Oscillations, Dynamical Systems, and Bifurcations of Vector Fields*, Springer, Berlin, 1986.
[5] L. Hsu, Analysis of critical and post-critical behaviour of non-linear dynamical systems by the normal form method, Part I: normalisation formulae, *Journal of Sound and Vibration* 89 (1983) 169–181.
[6] L. Hsu, Analysis of critical and post-critical behaviour of non-linear dynamical systems by the normal form method, Part II: divergence and flutter, *Journal of Sound and Vibration* 89 (1983) 183–194.
[7] G. Iooss, D.D. Joseph, *Elementary Bifurcation and Stability Theory*, Springer, Berlin, 1980.
[8] C. Elphick, E. Tiraipegui, M.E. Brochet, P. Couillet, G. Iooss, A simple global characterization for normal forms of singular vector fields, *Physica D* 29 (1987) 95–127.
[9] L. Jezequel, C.H. Lamarque, Analysis of non-linear dynamical systems by the normal form theory, *Journal of Sound and Vibration* 149 (1991) 429–459.
[10] P. Yu, Computation of normal forms via a perturbation technique, *Journal of Sound and Vibration* 211 (1998) 19–38.
[11] Q. Bi, P. Yu, Computation of normal forms of differential equations associated with non-semisimple zero eigenvalues, *International Journal of Bifurcation and Chaos* 8 (1998) 2279–2319.
[12] G.A. Baker, P. Graves-Morris, *Padé Approximants*, Cambridge University Press, Cambridge, 1996.
[13] C. Brezinski, Extrapolation algorithms and Padé approximations: a historical survey, *Applied Numerical Mathematics* 20 (1983) 299–318.

[14] R. Hughes Jones, General rational approximants in *N*-variables, *Journal of Approximation Theory* 16 (1976) 201–233.
[15] R. Hughes Jones, G.J. Makinson, The generation of Chisholm rational approximants to power series in two variables, *Journal of Institute of Mathematical Applications* 13 (1974) 299–310.
[16] T.M. Cameron, J.H. Griffin, An alternating frequency/time domain method for calculating the steady state response of nonlinear dynamic, *Journal of Applied Mechanics* 56 (1989) 149–154.
[17] S.Y. Liu, M.A. Ozbek, J.T. Gordon, A nonlinear model for aircraft brake squeal analysis. Part 1: model description and solution methodology, *American Institute of Aeronautics and Astronautics Journal* 3 (1996) 406–416.
[18] M.H. Travis, Nonlinear transient analysis of aircraft landing gear brake whirl and squeal, *American Society of Mechanical Engineers Design Engineering Technical Conferences*, Vol. 3, 1995, pp. 1209–1216.
[19] R.A. Ibrahim, Friction-induced vibration, chatter, squeal and chaos: Part I—mechanics of contact and friction, *American Society of Mechanical Engineers Applied Mechanics Review* 47 (7) (1994) 209–226.
[20] R.A. Ibrahim, Friction-induced vibration, chatter, squeal and chaos: Part II—dynamics and modeling, *American Society of Mechanical Engineers Applied Mechanics Review* 47 (7) (1994) 227–253.
[21] D.A. Crolla, A.M. Lang, Brake noise and vibration—state of art, *Tribologie, Vehicle Tribology* 18 (1991) 165–174.
[22] J.T. Oden, J.A.C. Martins, Models and computational methods for dynamic friction phenomena, *Computer Methods in Applied Mechanics and Engineering* 52 (1985) 527–634.
[23] R.T. Spurr, A theory of brake squeal, *Proceedings of the Automotive Division and Institute of Mechanical Engineers* 1 (1961/1962) 33–40.
[24] C. Gao, D. Kuhlmann-Wilsdorf, D.D. Makel, The dynamic analysis of stick-slip, *Wear* 173 (1994) 1–12.
[25] R.P. Jarvis, B. Mills, Vibrations induced by dry friction, *Proceedings of the Institute of Mechanical Engineers* 178 (32) (1963/1964) 847–866.
[26] S.W.E. Earles, G.B. Soar, Squeal noise in disc brakes, *Proceedings of the Institute of Mechanical Engineers Conference on Vibration and Noise in Motor Vehicles*, Paper C100/71, 1971.
[27] Millner, An analysis of disc brake squeal, Society Automotive Engineer Paper 780332, 1978.
[28] M.R. North, A mechanism of disc brake squeal, *14th FISITA Congress*, Paper 1/9, 1972.
[29] A.F. D'Souza, A.H. Dweib, Self-excited vibrations induced by dry friction. Part 2: stability and limit-cycle analysis, *Journal of Sound and Vibration* 137 (2) (1990) 177–190.
[30] D.J. Feld, D.J. Fehr, Complex eigenvalue analysis applied to an aircraft brake vibration problem, *American Society of Mechanical Engineers, Design Engineering Technical Conferences*, Vol. 3, 1995, pp. 1135–1141.